IGNITION OF INITIALLY UNMIXED GASES AT STAGNATION REGION OF A BLUNT POROUS BODY

A THESIS

Presented to

The Faculty of the Division of Graduate

Studies and Research

By

Tran-Xuan Phuoc

In Partial Fulfillment

of the Requirements for the Degree

Master of Science in Mechanical Engineering

Georgia Institute of Technology

November, 1974

IGNITION OF INITIALLY UNMIXED GASES AT STAGNATION REGION OF A BLUNT POROUS BODY

Approved:

P. Durbetaki, Chairman

C. W. Gorton

S. V. Shelton

Date approved by Chairman: 11/19/1974

ACKNOWLEDGMENTS

The author would like to express his appreciation to everyone who directly and indirectly helped him to finish this work, especially Dr. P. Durbetaki who served as his thesis advisor and reading committee chairman, for his kindness and numerously valuable suggestions and advice. The author also wishes to thank Dr. S. V. Shelton and Dr. C. W. Gorton who served as members of the thesis reading committee. He also would like to thank Mr. K. Annamalai for his discussions on the numerical method.

At last, but not at least, the author also would like to express his appreciation to his mother, Mrs. Phan-thi-Thanh, for her lovely guidance, and Miss Soren S. for her lovely character.

TABLE OF CONTENTS

LIST OF TABLES

LIST OF ILLUSTRATIONS

Figure Page

SUMMARY

The primary objective of this work is to investigate the ignition of initially unmixed gases at the stagnation region of a blunt porous body. With general assumptions of laminar boundary layer approximation together with the assumption that a second order Arrhenius law describes the chemical process, the governing equations were solved numerically to obtain the ignition characteristics of the flow by examining the surface heat transfer as a function of the First Damkohler Number. For various wall temperatures and injection rates the results showed that two types of transition can be obtained and the type of transition depends on the injection rate as well as the wall temperature. The curves for $Nu/(Re)^{1/2}$ and $\alpha_{F,w}$ as a function D_1, with $\bar{f}_w$ as a parameter, were used to obtain ignition and extinction conditions. Using the critical Damkohler Numbers of $D_{1,i}$ and $D_{1,e}$ the multi-valued transition solutions were divided into three regions to obtain three branch solutions.

The effect of wall temperature and injection rate were examined and have shown that the fuel mass fraction at the wall is a function of f_w, θ_w and D_1.

NOMENCLATURE

a	potential flow coefficient
A	frequency factor
C	$\rho\mu/\rho_e\mu_e$
C_p	specific heat at constant pressure
C_v	specific heat at constant volume
D	diffusion coefficient
D_{ij}	binary diffusion coefficient of species i through j
$D_{T,i}$	thermal diffusion coefficient of species i
D_1	First Damkohler Number, $A\rho_e/2a$
D_2	Second Damkohler Number, $q^\circ/C_pT_e\nu_FM_F$
$D_{1,i}$	Ignition First Damkohler Number
$D_{1,e}$	Extinction First Damkohler Number
E	activation energy
E^*	E/RT_e, dimensionless activation energy
f_i	external force per unit mass of species i
$\bar{f}_w$	blowing velocity, equation (3.65b)
h	specific enthalpy of mixture
h_c	heat convection coefficient
h_i	specific enthalpy of formation of species i
k	reaction rate constant
M_i	molecular weight of species i
N_i	number of mole of species i
Nu	Nusselt Number, $h_c\ x/\lambda$

Pr	Prandtl Number, $\mu C_p/\lambda$
$\vec{P}$	hydrostatic pressure
p	thermodynamic pressure
$\vec{q}$	heat flux vector
q°	heat of reaction
R	universal gas constant
Re	Reynolds Number, equation (4.6)
r_s	stoichiometric ratio
Sc	Schmidt Number, $\mu/\rho D$
T	absolute temperature
T_{max}	maximum temperature
u	internal energy of mixture
V	volume of mixture
$\vec{V}$	center mass velocity
$\vec{V}_i$	diffusion velocity of species i
$\vec{V}_j$	diffusion velocity of species j
x	distance along the surface
X	equation (4.31a)
X_j	mole fraction of species j
y	distance normal to the surface
Y	equation (4.31a)
Y_i	mass fraction of species i
Z	equation (4.31a)
α	thermal diffusivity
α_F	dimensionless fuel mass fraction, $Y_F/(Y_{F,w})_f$
α_N	equation (4.19)

β_F equation (4.13)

β_O equation (4.16)

$\delta_1 \ldots \delta_6$ equation (4.33)

$\Delta X, \Delta Y, \Delta Z$ correction for X, Y, Z

η Lee's transformation, $(\frac{2\rho_e a}{\mu_e})^{1/2} \int_o^\infty \frac{\rho}{\rho_e} dy$

θ dimensionless temperature, T/T_e

κ bulk viscosity coefficient

λ thermal conductivity

μ viscosity coefficient

ν_i stoichiometric coefficient of species i

ν_i' stoichiometric coefficient of species i appearing as reactant

ν_i'' stoichiometric coefficient of species appearing as product

ξ Lee's transformation, $\frac{\rho_e \mu_e a x^4}{4}$

ρ mixture density

τ_{ij} stress tensor

ϕ equation (4.10)

ψ $(2\xi)^{1/2} f(\eta)$, stream function

ω reaction rate

ω_i mass production (or consumption) per unit volume and time of species i

Subscripts

e free stream condition

equil equilibrium flow

F fuel

f frozen flow

N	inert
O	oxygen
P	product
w	wall condition
x	x-component
X	derivative with respect to X
y	y-component
Y	derivative with respect to Y
Z	derivative with respect to Z
UB	unburnt state
(c)	due to conduction
(d)	due to diffusion
(g)	under influences of body forces
(P)	under influence of pressure gradient
(r)	by radiation
(T)	of thermal diffusion
(x)	diffusion of concentration

CHAPTER I

INTRODUCTION

The process of burning of initially unmixed fuel is quite important in many branches of modern technology. Study of the ignition process is necessary because it is a process by which a propagating flame is originated and, therefore, a good understanding of the ignition process is quite helpful for the design of ramjet burners, rocket combustion chambers and for the prevention of explosion hazard in mines and industries.

Fuel can be ignited by several methods. Premixed fuel can be ignited by an electrical spark, by a small pilot flame or by heated surfaces. Ignition studies of the premixed category have been well understood. Ignition studies were made in the boundary layer of a combustible mixture over a flat plate or a blunt body, by which the characteristic length for stabilization of a flame in the case of the flat plate and the ignition temperature for the blunt body were obtained.

The process of combustion of initially unmixed fuel is carried out by supplying oxidizer and fuel individually. By that means, studies have been carried out successfully for the combustion of gas jet fuel, opposed jet diffusion

flame and the combustion of fuel droplets. In these studies the flame length as well as flame position were obtained. However, the ignition process of such a problem has not been well understood yet. Jain and Mukunda [1] investigated the ignition of the stream of oxidizer impinging on the porous wall where fuel was injected. Assuming incompressible flow they obtained some results which were considered to be a very good contribution to the combustion science. Recently Liu and Libby [2] and Wu and Libby [3] examined the problem similar to that but with hydrogen injection. Using a multistep reaction they reached the equilibrium state at a rather low First Damkohler Number and provided the single transition solution.

This thesis will deal with a similar problem. The hot surface of a blunt porous body is used. Oxidant mixture (oridizer plus inert) is flowing parallel to the axis of the body. Gaseous fuel is injected into the stagnation region of the boundary layer. The injected gas is at the same temperature as that of the wall (T_w) and higher than that of the oncoming stream. The main purpose of this thesis is to seek for the condition by which the combustible mixture can be ignited. Temperature and fuel mass fraction profiles are also established for the problem.

The basis for an ignition condition of a combustible mixture by hot surfaces can be referred to as the concept of minimum ignition energy [4]. The combustible mixture can be

ignited when the surface heat transfer to it exceeds the minimum value energy required for the mixture to be ignited. This condition exists when heat liberation by chemical reaction balances the rate of heat transfer from the surface so that the heat transfer from the surface is equal to zero. This statement is identified as the Van't Hoff criterion for ignition. The meaning of this is that when a combustible mixture approaches the hot surface, heat transfer from the surface results in bringing an increase in the temperature of the mixture which in turn increases the chemical reaction rate of the mixture. At the same time, during the approaching process, kinetic energy associated with the flowing mixture will convert into thermal energy. This energy will further increase the temperature and reduce net heat transfer from the surface. This consideration will lead to the conclusion that the concept of an adiabatic condition at the wall is an indication of self-heating process of the gaseous mixture by which the mixture has risen its temperature sufficiently to sustain chemical reaction. Using the Van't Hoff criterion one must visualize that the hot surface is a heat source, it can not absorb heat from the impinging stream so that when the temperature gradient becomes positive, ignition occurs. However, the surface can be maintained at an isothermal condition and the unignited state at low chemical conversion can persist even though a maximum temperature exists in the flowing mixture [5]. Therefore, it is not a

sufficient condition of ignition study but only an over-simplified approximation and can not be used to investigate the problem of ignition study exactly and at high ignition temperatures. At low ignition temperatures using the Van't Hoff criterion will give excellent results [6].

Because of the large deviation of the Van't Hoff criterion at high ignition temperatures, the ignition study has been suggested to examine the steady state solution of the governing equations from frozen to equilibrium flow. For a reactive flow, the First and Second Damkohler Numbers are used to describe the chemical process of the flow. The First Damkohler Number D_1 is defined as the ratio of convective time to chemical time while the Second Damkohler Number D_2 is the ratio of heat released by reaction to heat convected away.

In order to investigate the ignition phenomena, discussions will be focused on two assymtotic limiting cases of the chemically reacting flow in which at very small D_1 values the convective time is much faster than the chemical time and the gas particles do not have time to react; the system is in frozen condition. At very large D_1, chemical time is much faster than convective time, all gases diffusing to the reaction zone are consumed up and the system is in thermodynamic equilibrium. At intermediate D_1 values the system is physically unstable and will move towards the weak (very small D_1) or strong (very large D_1) burning [7].

Ignition is expected to occur as a transient process by which the system jumps from weak to strong burning. It was also discussed by Alkidas [8] that the transition from frozen to equilibrium of a chemically reacting flow affects the surface heat transfer. Heat transfer is a maximum for frozen and minimum for equilibrium flow, therefore, the phenomena of ignition should be governed by heat interacting at the surface and consequently the ignition study will require a knowledge of heat transfer from the surface. In this point of view, the Nusselt number describing the interface heat transport process should appear in the discussions and the problem reduces to investigating the effects of the degree of reaction on surface heat transfer.

With the short discussion above, it is clear that the ignition study can be carried out by investigation of the steady state solution of the conservation equations from frozen to equilibrium flow. The Nusselt and the First Damkohler Numbers must be used as obvious parameters for the ignition study.

The objectives of the present work are:

(i) to investigate the effects of the First Damkohler Number on the ignition and extinction conditions of initially unmixed gases at the stagnation region of a blunt body,

(ii) to study the effects of flow conditions and wall temperatures on the type of transition which occurs as the flow changes from frozen to equilibrium, and

(iii) to study the effects of flow conditions and wall temperature on the ignition temperature.

In order to carry out this analysis the set of governing equations will be written in two-dimensional axisymmetric form for the boundary layer at the stagnation region. Including compressible flow consideration, the coupled equations will be solved numerically. Ignition conditions can be obtained by plotting the heat interaction at the surface and the fuel mass fraction at the wall with the First Damkohler Number as the independent parameter. The profiles of the temperature as well as of the fuel mass fraction will also be established and presented.

CHAPTER II

LITERATURE REVIEW

2.1 Introduction

In this chapter, only past investigations that have been focused on the influence of the First Damkohler Number on the ignition and extinction will be reviewed. Section 2.2 will deal with the ignition and extinction of a diffusion flame, and in Section 2.3 the ignition and extinction by hot surfaces of premixed reactants will be examined. Since the combustion problem for this study is the initially unmixed category, the literature review in the premixed category will include only those works which give valuable information for the present work.

2.2 Ignition and Extinction of a Diffusion Flame

Dealing with the combustion problem of initially unmixed gases, Zeldovich [9] showed that the distribution of the concentrations of the products of combustion and the temperature for the combustion of initially unmixed gases are the same as for the combustion of a premixed stoichiometric mixture of the gases considered. The possible limit of the combustion of unmixed gases were also obtained and shown that it depends on the finite rate of chemical reaction and near the rate of combustion of a stoichiometric mixture.

Marble and Adamson [10] used series expansion techniques for a laminar mixing zone. They established the condition under which reaction enters a balance of diffusion and convection, and ignition occurs.

Spalding [11] in the problem of an opposed jet diffusion flame investigated the flow pattern, mixing pattern and the flame position and showed that the jet flow rate at extinction is independent of the transport properties. The burning rate and the flame location were obtained analytically.

Fendell [7] investigated the ignition and extinction in combustion of initially unmixed reactants between frozen and equilibrium conditions, he used the inner and outer expansion method to obtain the two asymptotic limits. For intermediate D_1 values a numerical method was used to show that the system in the middle branch is unstable, it is rarely observed and it will move towards the weak or strong burning branch. Ignition occurs when the system jumps from the weak to the strong branch. This occurs when D_1 increases for a system on the frozen flow branch. For a system on equilibrium flow branch, as D_1 decreases, under sufficiently strong perturbation, it crosses suddenly to the weak or frozen flow branch; this is extinction. By this interpretation, Fendell showed numerically for an ethanol-air mixture that the maximum temperature is a function of D_1 and also he obtained the ignition and extinction condition for the mixture by plotting T_{max} versus D_1.

Jain and Mukunda [1] studied the problem of ignition and extinction in a forced convection system, using the incompressible approximation with Prandtl and Schmidt numbers taken to be unity. They investigated the effects of wall temperature and activation energy on the ignition and extinction for an ethane-air mixture. Ignition and extinction were obtained by plotting the gradient of oxidant concentration at the origin versus D_1. It was shown that this method is equivalent to that of Fendell. However, there exist certain limits of temperature at the wall, beyond which the sharp extinction can not be distinguished. The flow speed at which extinction occurs increases with increasing wall temperature and the value of the Extinction Damkohler Number increases exponentially as activation energy increases. Similarly, Liu and Libby [2] and afterward Wu and Libby [3], using hydrogen injection, solved the problem with multistep reaction and they used a quasilinearization method to find a simple transition solution from frozen to equilibrium flow.

Polymeropoulos and Peskin [12] investigated the problem of ignition and extinction of liquid fuel drops. In this study, ignition was defined as the transient process from kinetic to diffusion control and extinction was a reverse transient process. Ignition and extinction conditions were obtained numerically as function of ambient oxygen concentration for various reaction rate, reaction order and stoichiometric ratios.

Marathe and Jain [13] with the problem of two opposed jets of equal diameter and a general Lewis Number showed that the gases with high Lewis Number should be more acceptable for flame stabilization where a high extinction velocity is required. Small Lewis numbers ought to be preferable for transpiration cooling where extinction velocity should be as small as possible. The ignition temperature is the characteristic condition which separates the solution into frozen and equilibrium regions and, therefore, there should be a discontinuity which occurs as the flow moves from frozen to equilibrium.

2.3 Ignition and Extinction of Premixed Reactants by Hot Surfaces

Past investigations on the ignition and extinction of premixed gases by hot surfaces with the First Damkohler Number as a parameter have been carried out by two methods: (i) an approximate method in which the Van't Hoff criterion must be used, and (ii) an absolute method in which ignition is defined as the transition process from frozen to equilibrium flow for the chemically reacting mixture. Sharma and Sirignano [14] using a quasilinearization method investigated the problem of ignition of stagnation point flow by hot body. The mixture was propane and air in stoichiometric proportion at T_e = 300°K and 1atm. A second order Arrhenius law of chemical reaction was assumed and the equations were solved

numerically. Their results showed that the ignition temperature decreases when D_1 increases. The effects of transport parameters such as Pr and Sc were also investigated and have shown that they are relatively minor.

Alkidas and Durbetaki [15] investigated the ignition characteristics for a cold combustible mixture of methane-air in stoichiometric proportion at the forward stagnation of a constant temperature plate. Using the formulation similar to that of Sharma and Sirignano, they found that fuel mass fraction at the wall decreases with decreasing D_1. The effects of activation energy, inert mass fraction, and temperature in the free stream on the ignition temperature were also investigated. Their general results were in agreement with those reported by Sharma and Sirignano. They also obtained the Critical First Damkohler Number, beyond which no ignition is possible.

Smith and Schmitz [5] focused their discussions mainly on the extinction phenomena of carbon monoxide-humid air mixture, three steady state solutions were obtained with the use of the Burke-Schuman approximation for the burning state (stable), of iterative procedures for extinguished state (stable), and of iterative numerical procedures for the intermediate state (unstable). Ignition was defined as the transition from steady operation at an extinguished state to steady operation at a burning state. Extinction follows in the opposite direction. The ignition characteristics

were also discussed and they have shown that the unignited state at low chemical conversion can persist even though a maximum temperature exists in the flowing mixture. Their result is in contrast with that from ignition study using the Van't Hoff criterion, in which ignition is considered to occur whenever $(\frac{\partial T}{\partial \eta})_{\eta=o} = 0$. A comparison of the Van't Hoff criterion at $T_w = 800°F$ with the absolute method indicated a prediction of the ignition velocity with the latter to be almost two times less than that obtained using Van't Hoff criterion. Unsteady solutions were also obtained and they have shown that, as with the results from the steady solution, the burning state and extinguishment are stable at least to small perturbation.

Alkidas and Durbetaki [16] using a methane-air mixture, investigated the effect of D_1 on the stagnation heat transfer with the absolute method and incompressible approximation. Their results indicated that the surface heat transfer rate is multi-value for a range of D_1 values and it becomes independent of D_1 and the wall temperature for values of D_1 up to 10^6. The First Ignition Damkohler Number is a strong function of the wall temperature. Recently, Alkidas and Durbetaki [6] compared the Critical Ignition Damkohler Number predicted by both the absolute method and the approximate method. Their results are somewhat different from those reported in reference [5]. However, corresponding to a given First Damkohler Number they showed that using the

approximate method will give excellent results of ignition temperature especially at low ignition temperatures.

CHAPTER III

FORMULATION OF THE PROBLEM

3.1 Introduction

In the analysis of many combustion problems, discussions can be confined in a one-dimensional flame front because the thickness of a laminar combustion zone is so thin that the flame front can be approximated as a plane in spite of the fact that it is curved. However, this approximation is not valid when the problem involves a thermal jet propulsion system, the ignition of a gaseous mixture by hot surfaces, or a thermal quenching near a cool wall. Such systems require a consideration beyond the one-dimensional flame front and can be confined in a two-dimensional field. They can be considered to behave very close to the boundary layer theory. Therefore the present problem should be formulated as a two-dimensional laminar boundary layer flow rather than a one-dimensional flame front.

In this chapter mathematical expressions describing the behavior of the system are developed. These expressions are confined to present

(i) an expression of fluid mechanical development in the two-dimensional axisymmetric boundary layer,

(ii) an expression of thermal development in the

boundary layer, and

(iii) an expression of the mixing pattern of the chemically reacting species.

It is necessary that these forms should be reduced, for the purpose of this thesis, to obtain exact solutions without sacrificing the physical interpretation. Consequently numerous assumptions and discussions will be given in Section 3.4. In Section 3.6 the chemical kinetic model will be discussed and the needed transformation presented in Section 3.7.

3.2 Flow Configuration

As shown in Figure 1 an oxidizing mixture of known temperature and composition approaches the non-catalytic surface of the axisymmetric blunt porous body situated at $y = 0$; its axis is parallel to the oncoming flow. The stream then divides and flows over the surface of the body. Pure fuel is injected, through the porous wall of the solid, into the boundary layer at the stagnation point region. The injected gases are at the same temperature as the wall T_w. The wall temperature is known and it is higher than that of the oncoming stream. The distances normal to and along the surface are represented by y and x, respectively. The radius of the surface is designated as r_o.

3.3 General Governing Equations

The fundamental governing equations for a multi-component

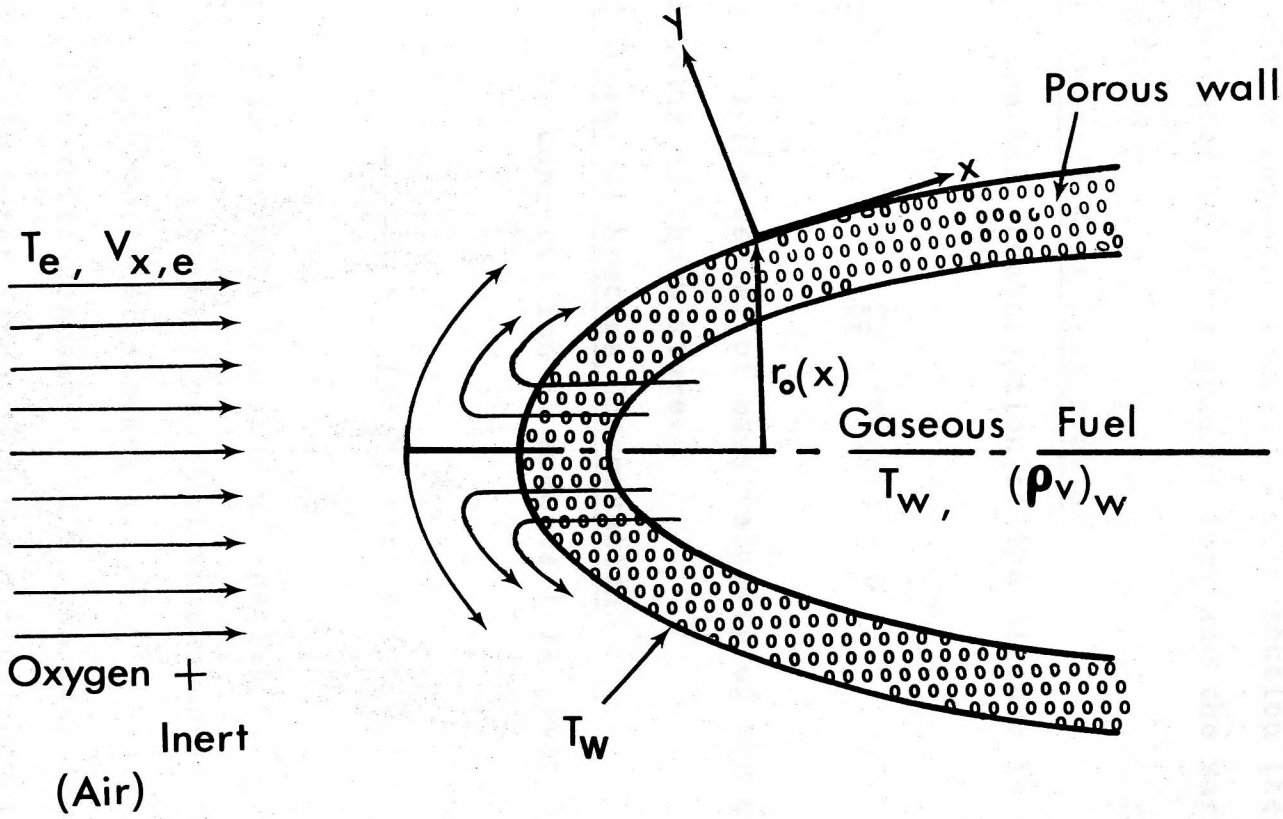

Figure 1. Flow Representation

reactive flow have been derived and presented in several references [4,17,18,19,20,21]. Details of these derivations will not be repeated here. In this section these equations are presented in their general form and the various terms are defined.

3.3.1 Overall Mass Conservation

The mass conservation of the mixture is given by

$$\frac{\partial \rho}{\partial t} + \nabla \cdot (\rho \vec{V}) = 0 \qquad (3.1)$$

where $\vec{V}$ is the center of mass velocity of the mixture; ρ is the density of the mixture.

3.3.2 Chemical Species Conservation

The conservation of species i is given by

$$\frac{\partial (\rho Y_i)}{\partial t} + \nabla \cdot (\rho Y_i \vec{V}) = \omega_i - \nabla \cdot (\rho Y_i \vec{V}_i) \qquad (3.2)$$

where Y_i is the mass fraction of species i; ω_i is the mass production of species i per unit volume and time; $\vec{V}_i$ is the diffusion velocity of species i.

In a multi-component fluid, the mass flux is influenced by the Soret Effect and the diffusion velocity can be written [22]:

$$\vec{V}_i = \vec{V}_i^{(x)} + \vec{V}_i^{(P)} + \vec{V}_i^{(g)} + \vec{V}_i^{(T)} \qquad (3.3)$$

where

$\vec{V}_i^{(x)}$ is the diffusion velocity of species i due to a concentration gradient, also called "ordinary diffusion velocity,"

$\vec{V}_i^{(P)}$ is the diffusion velocity of species i due to the influence of a pressure gradient imposed on the system,

$\vec{V}_i^{(g)}$ is the diffusion velocity of species i due to the difference of external forces acting on individual species,

$\vec{V}_i^{(T)}$ is the diffusion velocity of species i due to the influence of a temperature gradient.

3.3.3 Momentum Conservation

The general equation of motion is

$$\frac{\partial}{\partial t}(\rho\vec{V}) + \nabla\cdot(\rho\vec{V}\vec{V}) = -\nabla\vec{p} - \nabla\cdot\vec{\tau}_{ij} + \rho\sum_i^N Y_i\vec{f}_i \qquad (3.4)$$

where:

$\rho\sum Y_i\vec{f}_i$ represents the body forces,

$\vec{P}$ is the hydrostatic pressure tensor,

$\vec{\tau}_{ij}$ is the stress tensor, represents the viscous part of momentum flux.

In equation (3.4) the difference between a pure fluid flow and multi-component flow is only in the last term, this term accounts for the different external forces acting on each species.

3.3.4 Energy Equation

The general form of the energy equation is

$$\rho \frac{\partial u}{\partial t} + \rho\vec{V}\cdot\nabla u = -\nabla\cdot\vec{q} - P\nabla\cdot\vec{V} + \vec{\tau}_{ij}:\nabla\vec{V} + \rho \sum_{1}^{N} Y_i \vec{f}_i \cdot \vec{V}_i \qquad (3.5)$$

where heat flux $\vec{q}$ depends on both the thermal gradient and driving forces (Dufour Effect) and is given

$$\vec{q} = \vec{q}^{(c)} + \vec{q}^{(d)} + \vec{q}^{(r)} + \vec{q}^{(T)} \qquad (3.6)$$

where

$\vec{q}^{(c)}$ is the heat flux by conduction and given by Fourier's Law,

$\vec{q}^{(d)}$ is the heat diffusion,

$\vec{q}^{(r)}$ is the radiative heat transfer,

$\vec{q}^{(T)}$ is the heat flux due to thermal diffusion,

$P\nabla\cdot\vec{V}$ is the change of energy due to compression,

$\vec{\tau}_{ij}:\Delta V$ is the change of energy due to dissipation,

$\rho\vec{V}\cdot\nabla u$ is the change of energy due to convection, and

$\rho\frac{\partial u}{\partial t}$ is the time rate of change of energy.

3.3.5 Constitutive Equations

(a) Stress Field

$$\vec{\tau}_{ij} = (\frac{2}{3}\mu - \kappa)\nabla\cdot\vec{V} - \mu[\nabla\cdot\vec{V} + (\nabla\cdot\vec{V})^T] \qquad (3.7)$$

where

μ is the viscosity coefficient,

κ is the bulk viscosity coefficient,

$(\nabla\vec{V})^T$ is the transpose of the matrix.

(b) Heat Transfer Field

*Fourier's Law

$$\vec{q}^{(c)} = -\lambda\nabla T \tag{3.8a}$$

*Heat transfer by diffusion

$$\vec{q}^{(d)} = \rho\sum_i h_i Y_i \vec{V}_i \tag{3.8b}$$

*Heat transfer due to thermal diffusion

$$\vec{q}^{(T)} = RT \sum_i \sum_j X_j \frac{D_{T,i}}{M_i D_{ij}} (\vec{V}_i - \vec{V}_j) \tag{3.8c}$$

where

λ is the thermal conductivity,

T is the absolute temperature,

R is the universal gas constant,

D_{ij} is the binary diffusion coefficient of species i through j,

$D_{T,i}$ is the thermal diffusion coefficient of species i,

X_j is the mole fraction of species j,

M_i is the molal mass of species i,

$\vec{V}_j$ is the diffusion velocity of species j, and

h_i is the specific enthalpy of species i.

(c) Thermal Equation of State

$$P = \rho RT \sum_i (Y_i/M_i) \tag{3.9}$$

(d) Caloric Equation

$$h_i = h_i^o + \int_{T^o}^{T} C_{p,i}\, dT \tag{3.10}$$

where

h_i^o is the specific heat of formation of species i,

T^o is the reference temperature.

(e) Thermodynamic Relation

$$u = \sum_1^N h_i Y_i - P/\rho \tag{3.11}$$

(f) Fick's Law*

$$\vec{V}_i = -D_{ij} \nabla \mathrm{Ln}\, Y_i \tag{3.12}$$

3.4 Assumptions

The set of governing equations presented in the

*Valid only if D_{ij} for the chemical components are equal.

previous section is in highly general form. Fortunately, relations such as Soret and Dufour Effects as well as radiant heat transfer can be neglected in most combustion problems because their contributions are negligible. The effects of external forces were discussed briefly in reference [22] and they are considered to be of primary importance only in ionic system where the external forces on an ion are equal to the product of the ionic charge and the local electric field strength. Each species, therefore, may be under the influence of different forces. For the problem under consideration in this thesis, gravity force is the only external force, acting equally on the chemical species. Therefore, this term vanished from equations (3.3), (3.4) and (3.5). Pressure diffusion is important only when the system is under the effect of a centrifugal force, otherwise the tendency for the mixture to separate under pressure gradient is very small. Thermal diffusion is also quite small unless one needs to produce a very steep temperature gradient such as in the case of isotope separation or a separation of a complex mixture of a very similar organic compound.

Marble [10] discussed that the variation of temperature, velocity and composition is considerably larger in the direction normal to the stream than it is parallel to the flow when the combustion process involves thermal ignition by hot surface. This characteristic will lead to the boundary

layer approximation.

Based on the above discussion, the following assumptions are made:

(a) Boundary layer approximation is valid,

(b) Laminar steady flow exists in the region of interest,

(c) Fourier's Law and Fick's Law are valid,

(d) $D_{ij} = D_{FO} = D_{OF} = \ldots = D$,

(e) $C_{p,i} = C_{p,e} = C_p = \text{Constant}$,

(f) Low speed flow exists,

(g) Radiation is negligible,

(h) Soret and Dufour Effects are negligible,

(i) Body forces are negligible,

(j) Gases are ideal, and

(k) Viscous dissipation is negligible.

The bulk viscosity coefficient is identically zero only for low density monatomic gases and is not too important in dense gases and liquids. In multi-component fluid systems there exists the diffusion stress tensor due to the relative motion of the species but its contribution is negligible.

Assumption (j) leads to consideration that properties of an ideal gas can be expressed in terms of the temperature. Density is inversely proportional to the temperature when the gas velocity in laminar flow is very small compared to the velocity of sound. Viscosity can be treated as a linear function of local temperature. This assumption is good when

the combustible gases and the combustion products have nearly the same molecular weight. Density and viscosity can be expressed as

$$\frac{\mu}{\mu_e} = \frac{T}{T_e} \tag{3.13a}$$

$$\frac{T}{T_e} = \frac{\rho_e}{\rho} \tag{3.13b}$$

where subscript e represents the free stream condition, then

$$C = \frac{\mu\rho}{\mu_e\rho_e} = 1 \tag{3.14}$$

3.5 Compressible Boundary Layer Equations

3.5.1 Governing Equations

With the assumptions given in the previous section the general equations are reduced for the boundary layer.

(a) Overall Mass Conservation

Using assumptions (a), (b), equation (3.1) becomes

$$\frac{\partial}{\partial x}(\rho v_x x) + \frac{\partial}{\partial y}(\rho v_y x) = 0 \tag{3.15}$$

(b) Chemical Species Conservation

Using assumptions (a), (b), (e), (d) and (h), equation

(3.2) becomes

$$\rho v_x \frac{\partial Y_i}{\partial x} + \rho v_y \frac{\partial Y_i}{\partial y} = \omega_i + \frac{\partial}{\partial y} \left(\rho D \frac{\partial Y_i}{\partial y}\right) \tag{3.16}$$

for i = O,F,N, where O represents the oxidizer, F the fuel and N the inert gas. The source term for the inert gas is taken to be zero, i.e.

$$\omega_N = 0 \tag{3.17}$$

and the product conservation can be computed by

$$Y_P + Y_F + Y_O + Y_N = 1 \tag{3.18}$$

(c) Momentum Equation

Using assumptions (a), (b), (f) and (i), equation (3.4) becomes

$$\rho v_x \frac{\partial v_x}{\partial x} + \rho v_y \frac{\partial v_x}{\partial y} = - \frac{\partial P}{\partial x} + \frac{\partial}{\partial y} \left(\mu \frac{\partial v_x}{\partial y}\right) \tag{3.19}$$

and

$$\frac{\partial P}{\partial y} = 0 \tag{3.20}$$

The pressure in this equation relates to the free stream

velocity through the Bernoulli equation

$$\frac{P_e}{\rho_e} + \frac{V_{x,e}^2}{2} = \text{Constant} \tag{3.21}$$

From equation (3.20) it is clear that the pressure is uniform throughout the boundary layer, hence

$$\frac{P_e}{\rho_e} + \frac{V_{x,e}^2}{2} = \frac{P}{\rho_e} + \frac{V_{x,e}^2}{2} = \text{Constant} \tag{3.22}$$

where

$$V_{x,e} = ax \tag{3.23}$$

(d) Energy Equation

Using assumptions (a) through (k) and equation (3.6) equation (3.5) becomes

$$\rho\vec{V}\nabla u = \nabla[\lambda\nabla T - \rho\Sigma h_i Y_i \vec{V}_i] - P\nabla\cdot\vec{V} \tag{3.24}$$

Using equations (3.12), (3.10), (3.11) and (3.16), equation (3.24) becomes

$$\rho v_x C_p \frac{\partial T}{\partial x} + \rho v_y C_p \frac{\partial T}{\partial y} = \frac{\partial}{\partial y}\left(\lambda \frac{\partial T}{\partial y}\right) - \sum_1^N h_i \overset{\circ}{\omega}_i \tag{3.25}$$

3.5.2 Boundary Conditions

These above equations will be solved with the following boundary conditions

*Momentum Equation

$$\left.\begin{aligned} &\text{at } y = 0: && v_x = 0 \\ & && \rho v_y = (\rho v)_w \end{aligned}\right\} \quad (3.26a)$$

$$\text{as } y\to\infty: \qquad v_x \to V_{x,e} = ax \qquad (3.26b)$$

*Oxidizer

$$\text{at } y = 0: \qquad (\rho v)_w\, Y_{O,w} = \left[\rho D \frac{\partial Y_O}{\partial y}\right]_w \qquad (3.27a)$$

$$\text{as } y\to\infty: \qquad Y_O \to Y_{O,e} \qquad (3.27b)$$

*Fuel

$$\text{at } y = 0: \qquad (\rho v)_w [Y_{F,w} - 1] = \left[\rho D \frac{\partial Y_F}{\partial y}\right]_w \qquad (3.28a)$$

$$\text{as } y\to\infty: \qquad Y_F \to 0 \qquad (3.28b)$$

*Inert

$$\text{at } y = 0: \qquad (\rho v)_w\, Y_{N,w} = \left[\rho D \frac{\partial Y_N}{\partial y}\right]_w \qquad (3.29a)$$

as $y \to \infty$: $$Y_N \to Y_{N,e} \tag{3.29b}$$

*Energy

at $y = 0$: $$T = T_w \tag{3.30a}$$

as $y \to \infty$: $$T \to T_e \tag{3.30b}$$

where subscript w indicates the condition at the wall, e the condition in the free stream.

3.6 Reaction Kinetics Model

Mass production (or consumption) terms due to chemical reaction can be evaluated by the theory of reaction kinetics. The reaction mechanism of a flame is very complex because the true combustion involves a great number of elementary reaction between stable and unstable species. The overall chemical kinetics was introduced to approach the calculation of the source terms. This concept has been used in references [1,16,15] and it will also be used for the present work.

The reaction can be expressed by the following equation

$$\sum_{i=1}^{N} \nu_i' M_i \to \sum_{i=1}^{N} \nu_i'' M_i \tag{3.31}$$

where ν_i' is the stoichiometric coefficient of species i appearing as reactant; ν_i'' is the stoichiometric coefficient of species i appearing as product.

The mass production (or consumption) is defined as

$$\omega_i = M_i(\nu_i'' - \nu_i')\omega \tag{3.32}$$

then the reaction rate of the above equation is

$$\omega = \frac{\omega_i}{M_i(\nu_i'' - \nu_i')} \tag{3.33}$$

The reaction rate of a chemical reaction can be determined by Law of Mass Action [4]. It states that reaction rate is proportional to the collisions of appropriate molecules and the collisions are proportional to the concentration of species. This statement can be represented as

$$\omega = k \prod_{i=1}^{N} C_i^{\nu_i'} \tag{3.34}$$

where

C_i is the concentration of species,

k is the specific reaction rate constant

The specific reaction rate constant is given by the Arrhenius equation

$$k = Ae^{-E/RT} \tag{3.35}$$

in which E is activation energy, A is frequency factor. Both of these are discussed by Laider [23].

The mass production (or consumption) can be evaluated from

$$\omega_i = M_i(\nu_i'' - \nu_i')\omega \tag{3.36}$$

$$= M_i(\nu_i'' - \nu_i')Ae^{-E/RT} \prod_1^N C_i^{\nu_i} \tag{3.37}$$

For the present work the assumption is made that the chemical reaction is complete, second order, single step and irreversible. All reactants diffuse to the reaction zone at the rate for the stoichiometric ratio to obey the following equation

$$\nu_O M_O + \nu_F M_F + \nu_N M_N \rightarrow \nu_P M_P + \nu_N M_N \tag{3.38}$$

From this equation it is clear that there exists a relation between all reacting species concentrations.

The source terms, therefore, can be computed by using equation (3.37) with:

$$\left.\begin{aligned} \nu_i'' &= 0; \text{ for } i = O,F \\ \nu_i'' &= \nu_P, \nu_N \end{aligned}\right\} \tag{3.39a}$$

$$\left.\begin{aligned} \nu_i' &= 0; \text{ for } i = P \\ \nu_i' &= \nu_F, \nu_O, \nu_N \end{aligned}\right\} \quad (3.39b)$$

and molecular concentration is

$$C_i = \frac{M_i}{V} = \rho Y_i \quad (3.40)$$

then

$$\omega = -\frac{\omega_F}{\nu_F M_F} = -\frac{\omega_O}{\nu_O M_O} = \frac{\omega_P}{\nu_P M_P} \quad (3.41)$$

or

$$\omega_O = -A\rho^2 \nu_O M_O Y_O Y_F e^{-E/RT} \quad (3.42)$$

$$\omega_F = -A\rho^2 \nu_F M_F Y_O Y_F e^{-E/RT} \quad (3.43)$$

$$\omega_P = +A\rho^2 \nu_P M_P Y_O Y_F e^{-E/RT} \quad (3.44)$$

Generally, this consideration is not valid because reaction is not a single step and in one direction, but if the temperature is not too high the reverse reaction can be neglected and these expressions for the source terms are

adequate for the present analysis.

3.7 Similarity Transformation

In order to transfrom the set of governing equations into the set of ordinary differential equations Lee's transformation parameters are used [24]

$$\eta = \left(\frac{2\rho_e a}{\mu_e}\right)^{1/2} \int_0^y \frac{\rho}{\rho_e}\, dy \tag{3.45a}$$

$$\xi = \frac{\rho_e \mu_e a x^4}{4} \tag{3.45b}$$

and the stream function is defined

$$\psi(\xi,\eta) = (2\xi)^{1/2} f(\eta) \tag{3.46}$$

where

$$f'(\eta) = \frac{v_x}{V_{x,e}} \tag{3.47}$$

The x-y coordinates are transformed to ξ-η coordinates by means of the following relations

$$\frac{\partial}{\partial y} = \left(\frac{2\rho_e a}{\mu_e}\right)^{1/2} \frac{\rho}{\rho_e} \frac{\partial}{\partial \eta} \tag{3.48a}$$

$$\frac{\partial}{\partial x} = \rho_e \mu_e a x^3 \frac{\partial}{\partial \xi} \tag{3.48b}$$

Thus

$$\rho v_x x = \frac{\partial \Psi}{\partial y} \tag{3.49a}$$

$$\rho v_y x = - \frac{\partial \Psi}{\partial x} \tag{3.49b}$$

satisfies the overall mass conservation automatically. By equation (3.48a)

$$\rho v_y x = - \frac{\partial \Psi}{\partial \xi} \frac{d\xi}{dx}$$

$$= - (2\rho_e \mu_e a)^{1/2} x f(\eta)$$

or

$$\rho v_y = - (2\rho_e \mu_e a)^{1/2} f(\eta) \tag{3.50}$$

3.7.1 Transformed Equations

(a) Momentum Conservation

Using equations (3.13b), (3.14), (3.22), 3.23), (3.47), (3.48a), (3.48b) and (3.50), equation (3.19) becomes

$$f''' + ff'' = \frac{1}{2} [f'^2 - \theta] \tag{3.51}$$

(b) Oxidizer Conservation

Using equations (3.14), (3.42), (3.48a) and (3.50), equation (3.16) for the oxidizer becomes

$$(\frac{1}{Sc} Y_O')' + fY_O' = \frac{A\rho\nu_O M_O Y_O Y_F e^{-E/RT}}{2a} \tag{3.52}$$

(c) Fuel Conservation

Using equations (3.14), (3.43), (3.48a) and (3.50), equation (3.16) for the fuel becomes

$$(\frac{1}{Sc} Y_F')' + fY_F' = \frac{A\rho\nu_F M_F Y_O Y_F e^{-E/RT}}{2a} \tag{3.53}$$

(d) Inert Conservation

Using equations (3.14), (3.43), (3.48a), (3.17) and (3.50), equation (3.16) for the inert becomes

$$(\frac{1}{Sc} Y_N')' + fY_N' = 0 \tag{3.54}$$

(e) Energy Conservation

Using equations (3.14), (3.42), (3.43), (3.44), (3.48a) and (3.50), equation (3.25) becomes

$$(\frac{1}{Pr} T')' + fT' = \frac{-A\rho q^o Y_O Y_F e^{-E/RT}}{2aC_p} \tag{3.55}$$

where prime indicates differentiation with respect to η and

$$\text{Sc: Schmidt Number} = \mu/\rho D \tag{3.56}$$

$$\text{Pr: Prandtl Number} = \mu C_p/\lambda \tag{3.57}$$

$$q^o = h_F^o \nu_F M_F + h_O^o \nu_O M_O - h_P^o \nu_P M_P \tag{3.58}$$

Define

$$\theta = \frac{T}{T_e} \tag{3.59}$$

$$D_1 = \frac{A\rho_e}{2a} \tag{3.60a}$$

$$D_2 = \frac{q^o}{C_p T_e \nu_F M_F} \tag{3.60b}$$

then with equation (3.13b), equations (3.52) through (3.55) can be rewritten

*Oxidizer Conservation

$$(\frac{1}{Sc} Y_O')' + fY_O' = \frac{D_1 \nu_O M_O Y_O Y_F e^{-E^*/\theta}}{\theta} \tag{3.61}$$

*Fuel Conservation

$$(\frac{1}{Sc} Y_F')' + fY_F' = \frac{D_1 \nu_F M_F Y_O Y_F e^{-E^*/\theta}}{\theta} \tag{3.62}$$

*Inert Conservation

$$(\frac{1}{Sc} Y_N')' + fY_N' = 0 \tag{3.63}$$

*Energy Conservation

$$(\frac{1}{Pr} \theta')' + f\theta' = \frac{-D_1 D_2 \nu_F M_F Y_O Y_F e^{-E^*/\theta}}{\theta} \tag{3.64}$$

where $E^* = E/RT_e$ is the dimensionless activation energy.

3.7.2 Transformed Boundary Conditions

(a) Momentum Conservation

at $\eta = 0$: $$f'(0) = 0 \tag{3.65a}$$

$$(\rho v)_w = -(2\rho_e \mu_e a)^{1/2} f(0) \tag{3.65b}$$

$$f(0) = -\frac{(\rho v)_w}{(2\rho_e \mu_e a)^{1/2}} = \bar{f}_w = \text{const} \tag{3.65c}$$

where v_w is the wall injection velocity of fuel; then $\bar{f}_w$ represents the blowing velocity parameter,

as $\eta \to \infty$: $$f'(\infty) \to 1.0 \tag{3.65d}$$

(b) Oxidizer Conservation

at $\eta = 0$: $$Y_{O,w} = -\frac{1}{Sc}\frac{1}{\bar{f}_w} Y_O'(0) \tag{3.66a}$$

as $\eta \to \infty$: $$Y_O \to Y_{O,e} \tag{3.66b}$$

(c) Fuel Conservation

at $\eta = 0$: $$(Y_{F,w}-1) = -\frac{1}{Sc}\frac{1}{\bar{f}_w} Y_F'(0) \tag{3.67a}$$

as $\eta \to \infty$: $$Y_F \to 0 \tag{3.67b}$$

(d) Inert Conservation

at $\eta = 0$: $$Y_{N,w} = -\frac{1}{Sc}\frac{1}{\bar{f}_w} Y_N'(0) \tag{3.68a}$$

as $\eta \to \infty$: $$Y_N \to Y_{N,e} \tag{3.68b}$$

(e) Energy Conservation

at $\eta = 0$: $$\theta = \frac{T_w}{T_e} = \theta_w \tag{3.69}$$

as $\eta \to \infty$: $$\theta = \frac{T_e}{T_e} \to 1 \tag{3.69b}$$

CHAPTER IV

STEADY STATE SOLUTION

4.1 Introduction

In this chapter the procedures used to solve the conservation equations numerically will be discussed. The numerical method used is presented in Section 4.5. However, before proceeding with the computer calculations, in order to reduce the number of equations required to be solved, some additional mathematical operations have been carried out and these are given in Section 4.4.

The calculations are confined mainly on investigating the effect of the wall temperatures and flow conditions on the type of transition achieved when moving from frozen to equilibrium flow, and to establish the ignition conditions.

4.2 General Theory

There are three main aspects involved with the present problem as discussed in Chapter III. Therefore, the solution that is sought must be such that the three aspects are satisfied. For fluid mechanical development over a blunt body with blowing, the solution is available in the literature. For the chemical species mass fraction and the development of temperature from frozen to equilibrium

flow, the solutions have been classified into two categories: simple transition and multi-transition as shown in Figures 2a and 2b, respectively. The type of transition, therefore, is not unique and depends strongly on the type of fuel and the conditions to which the combustion process is exposed. From these figures it is clear that when $(D_1)_{equil} >> (D_1)_f$ simple transition exists. However, as soon as $(D_1)_{equil} << (D_1)_f$ multi-transition will be obtained. Therefore, D_1 should be an obvious parameter to be used to determine the type of solution.

However, one must recognize that D_1 was defined basically by reference properties known a priori. It is, therefore, only a true indication of the ratio of overall resident time to reaction time in the boundary layer, when the reaction is dissociation or recombination. The ignition study mainly deals with the problem of a strong exothermic reaction. The temperature of the reaction zone, therefore, increases greatly from its original value without reaction, and the exponential function of the local Damkohler Number varies drastically [25]. Under these conditions D_1 is not a true indication of resident time to chemical time ratio in the main reaction zone. In this case, another parameter should be introduced to describe the degree of the reactivity in the boundary layer. It was discussed briefly in Chapter I that the transport processes at the interface are important for such a problem. These processes are the heat transport

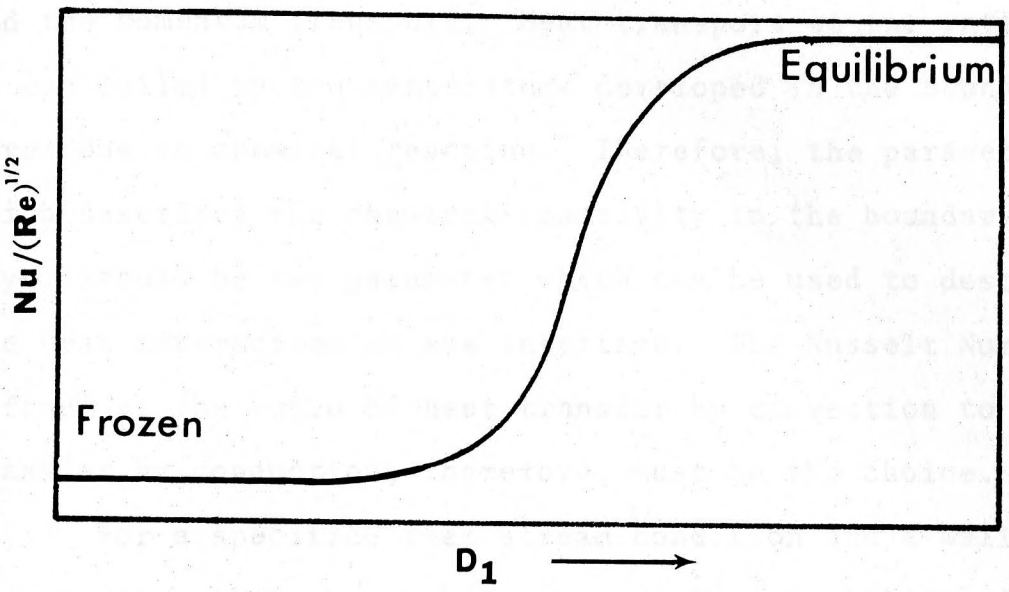

Figure 2a. Simple Transition Representation

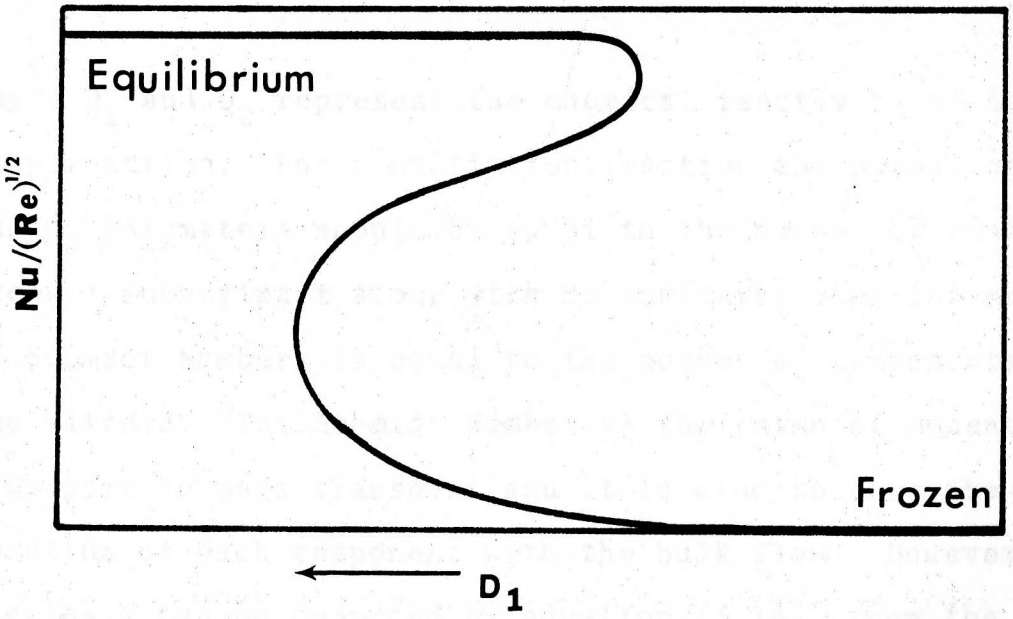

Figure 2b. Multi-Transition Representation

and the momentum transport. Heat transport at the interface is controlled by the temperature developed in the boundary layer due to chemical reaction. Therefore, the parameter which describes the chemical reactivity in the boundary layer should be the parameter which can be used to describe the heat interaction at the interface. The Nusselt Number defined as the ratio of heat transfer by convection to heat transfer by conduction, therefore, must be the choice.

For a specified free stream condition and a wall temperature, the general solution, derived by Alkidas [8], can be modified and taken as

$$\theta = \theta[D_1, D_2, Nu, Re, Pr, (Sc)_i, \bar{f}_w, \eta] \tag{4.1}$$

where D_1 and D_2 represent the chemical reactivity of a single step reaction. For a multi-step reaction the number of D_1 and D_2 parameters should be equal to the number of reaction steps. Subscript i along with Sc indicates that the number of Schmidt Numbers is equal to the number of components in the mixture. The Schmidt Number is the ratio of momentum transport to mass transport and it is used to describe the relation of each component with the bulk flow. However, species N can be computed by equation (3.18), then the subscript i will run from 1 to N-1 only. Parameter $\bar{f}_w$ represents the blowing velocity at the wall required in the solution in order to describe the flow condition as the rate

of injection, which dominates the mixing pattern in the boundary layer. The higher the injection rate the higher the quantity of fuel at the surface which in turn requires more oxygen. This leads to a condition whereby ignition occurs at very low D_1 and far away from the wall where the mixing is assumed to be in stoichiometric proportions. At low rate of injection, fuel at the wall will be in small quantity and the reaction zone is almost at the wall. The reaction goes to equilibrium with a simple transition due to the lack of fuel for the middle branch to exist.

4.3 Derivation of Nusselt Number

It was discussed before that the surface heat transfer depends strongly on the degree of reactivity in the boundary layer. The mechanism of heat transfer for this problem is very complex, therefore, it is desirable to examine the surface heat transfer in the region between the two limiting cases of the chemical reaction. In the frozen flow regime no reaction is observed to occur and the transport in the boundary layer is mainly controlled by the diffusion rate. Heat transfer from the surface to the boundary layer is accomplished partly by conduction and partly by diffusion of the chemical species. In equilibrium flow chemical reaction is very fast and gas particles are in their equilibrium values appropriate to the local temperature at every point of the flow. The actual physical situation is

expected to be somewhere between the above two limits [24].

In order to describe the heat transfer in this regime the Nusselt Number is derived by calculating the heat conduction at the wall due to the temperature gradient developed in the boundary layer by chemical reaction. It is given as

$$q_w = - \lambda \left(\frac{\partial T}{\partial y}\right)_w \tag{4.2a}$$

and in η coordinate

$$q_w = - \left(\frac{2\rho_e a}{\mu_e}\right)^{1/2} \frac{\rho}{\rho_e} \lambda \left(\frac{dT}{d\eta}\right)_w \tag{4.2b}$$

Using the dimensionless temperature introduced by equation (3.59), equation (4.2b) becomes

$$q_w = - \left(\frac{2\rho_e a}{\mu_e}\right)^{1/2} \frac{\rho}{\rho_e} T_e \lambda \left(\frac{d\theta}{d\eta}\right)_w \tag{4.3}$$

but

$$q_w = h_c (T_e - T_w) \tag{4.4}$$

where h_c is the convective film coefficient. The Nusselt Number is given by

$$Nu = \frac{h_c x}{\lambda} = \frac{q_w x}{\lambda(T_e - T_w)} \tag{4.5}$$

and the Reynolds Number defined by

$$Re = \frac{\rho_w V_{x,e} x}{\mu_w} \tag{4.6}$$

Using equations (3.14), (4.3), (4.5) and (4.6), Nu can be expressed as

$$Nu/(Re)^{1/2} = \frac{-\sqrt{2}}{1-\theta_w} \left(\frac{d\theta}{d\eta}\right)_w \tag{4.7}$$

It should be noted that heat transfer is independent of the particular choice of reference density and viscosity, the use of wall density and wall viscosity is merely a convenience.

4.4 Intermediate Mathematical Operations

4.4.1 Combine Oxidizer and Fuel Conservation Equations

Let

$$r_s = \frac{\nu_O M_O}{\nu_F M_F} \tag{4.8}$$

where r_s is the stoichiometric ratio. Equations (3.61) and (3.62) can be combined to give

$$\frac{1}{Sc}\left[Y_F - \frac{Y_O}{r_s}\right]'' + f\left[Y_F - \frac{Y_O}{r_s}\right]' = 0 \qquad (4.9)$$

Defined the ϕ equation

$$\phi = \frac{(Y_F - Y_O/r_s) - (Y_F - Y_O/r_s)_e}{(Y_F - Y_O/r_s)_w - (Y_F - Y_O/r_s)_e} \qquad (4.10)$$

then equation (4.9) becomes

$$\phi'' + Sc\, f\phi' = 0 \qquad (4.11)$$

4.4.2 Combine Fuel and Energy Conservation Equations

Divide equation (3.64) by D_2 then add to equation (3.62) and assume that Lewis Number = 1 (i.e. Pr = Sc). The derivation gives

$$\left(\frac{\theta}{D_2} + Y_F\right)'' + f\,Pr(\theta/D_2 + Y_F)' = 0 \qquad (4.12)$$

Define β_F as

$$\beta_F = \frac{(Y_F + \theta/D_2) - (Y_F + \theta/D_2)_e}{(Y_F + \theta/D_2)_w - (Y_F + \theta/D_2)_e} \qquad (4.13)$$

then equation (4.12) becomes

$$(\beta_F)'' + f\,Pr\,(\beta_F)' = 0 \qquad (4.14)$$

4.4.3 Combine Oxidizer and Energy Conservation Equations

Oxygen and energy conservation equations can be combined and give

$$\left(\frac{Y_O}{r_s} + \frac{\theta}{D_2}\right)'' + fPr(Y_O/r_s + \theta/D_2)' = 0 \qquad (4.15)$$

Define β_O as

$$\beta_O = \frac{(Y_O/r_s + \theta/D_2) - (Y_O/r_s + \theta/D_2)_e}{(Y_O/r_s + \theta/D_2)_w - (Y_O/r_s + \theta/D_2)_e} \qquad (4.16)$$

then equation (4.15) becomes

$$(\beta_O)'' + f\,Pr\,(\beta_O)' = 0 \qquad (4.17)$$

Using the unburnt state of fuel at the wall as reference the fuel mass fraction can be written as

$$(\alpha_F)_{UB} = Y_F/Y_{F,w} \qquad (4.18a)$$

then

$$(\alpha_F)''_{UB} + fSc\,(\alpha F)'_{UB} = 0 \qquad (4.18b)$$

Similarly the inert gas mass fraction can be written as

$$\alpha_N = \frac{Y_N - Y_{N,e}}{Y_{N,w} - Y_{N,e}} \tag{4.19a}$$

then equation (3.63) becomes

$$\alpha_N'' + fSc\alpha_N' = 0 \tag{4.19b}$$

The defined equations have the following boundary conditions

at $\eta = 0$:

$$\left.\begin{array}{l} \phi(0) \\ (\alpha_{F,w})_{UB} \\ \alpha N,w \\ \beta_F(0) \\ \beta_O(0) \end{array}\right\} = 1 \tag{4.20a}$$

at $\eta \to \infty$

$$\left.\begin{array}{l} \phi(\infty) \\ (\alpha_F(\infty))_{UB} \\ \alpha_N(\infty) \\ \beta_F(\infty) \\ \beta_O(\infty) \end{array}\right\} \to 0 \tag{4.20b}$$

The solutions of these equations subjected to the above boundary conditions are similar and

$$\phi = \beta_F = \beta_O = \alpha_N = (\alpha_F)_{UB} \tag{4.21}$$

4.4.4 Coupled Relationships

From equations (4.13) and (4.21) the relation between Y_F and θ is given by

$$\frac{\theta}{D_2} = -Y_F - \phi[1/D_2 - (Y_F + \theta/D_2)_w] + 1/D_2 \tag{4.22}$$

Using equations (4.16) and (4.21), the relation between Y_O and θ is given by

$$\frac{\theta}{D_2} = \phi[(Y_O/r_s+\theta/D_2)_w - (Y_O/r_s+\theta/D_2)_e] + (Y_O/r_s+\theta/D_2)_e - Y_O/r_s \tag{4.23}$$

Finally using equations (4.10) and (4.21), the relation between Y_O and Y_F is given by

$$Y_F = \frac{Y_O}{r_s} - \frac{Y_{O,e}}{r_s} + \phi[(Y_F - Y_O/r_s)_w + \frac{Y_{O,e}}{r_s}] \tag{4.24}$$

Expression for $Y_{O,w}$ can be obtained by using the boundary conditions (3.66a) and (3.67a)

$$Y_{F,w} = \frac{Y_{O,w}}{r_s} + \frac{Sc\bar{f}_w - \phi'(0)Y_{O,e}/r_s}{Sc\bar{f}_w + \phi'(0)} \tag{4.25}$$

From equation (4.25) one can obtain an expression for $Y_{F,w}$ for the thin flame theory (i.e. $Y_{O,w} = 0$)

$$Y_{F,w} = \frac{Sc\bar{f}_w - \phi'(0)Y_{O,e}/r_s}{Sc\bar{f}_w + \phi'(0)} \tag{4.26}$$

Also, from equation (4.25) the condition for which the fuel mass fraction at the wall becomes negative is

$$Sc\bar{f}_w < \frac{\phi'(0)[Y_{O,e} - Y_{O,w}]}{r_s + Y_{O,w}} \tag{4.27}$$

It is clear that the injection rate at which $Y_{F,w} = 0$, is lower for the case of finite chemical kinetics than the case of thin flame theory. The reason for $Y_{F,w} << 0$ can be understood because of low injection rate. The rate of fuel transfer and the rate of chemical reaction are such that all fuel is consumed at the interface. As soon as this condition occurs, homogeneous combustion is no longer valid and the assumption of heterogenous combustion must be taken into account.

The surface heat transfer can be calculated from equations (4.16) and (4.21), and is given by

$$Nu/(Re)^{1/2} = \frac{\sqrt{2}}{\theta_w - 1} \left[\phi'(0)\left(\frac{Y_{O,w}}{r_s} D_2 + \theta_w - 1 - \frac{Y_{O,e}}{r_s} D_2\right) - D_2 Y'_{O,w}/r_s\right] \tag{4.28}$$

where $Y_{O,w}$ and $Y'_{O,w}$ relates to each other by equation (3.66a).

For equilibrium $D_1 \to \infty$, then

$$Nu/(Re)^{1/2} = \frac{\sqrt{2}}{\theta_w - 1} \left[\phi'(0)\left(\theta_w - 1 - \frac{Y_{O,e}}{r_s} D_2\right)\right] \tag{4.29}$$

For frozen $D_1 \to 0$, and

$$Nu/(Re)^{1/2} = \sqrt{2}\ \phi'(0) \tag{4.30}$$

4.4.5 Method of Solution

The main purpose of this thesis is to seek for the solution with finite D_1. In order to do so, the set of coupled governing equations must be integrated simultaneously for various values of D_1 taken between frozen and equilibrium flow.

The equations to be solved are

(a) Momentum

$$f''' + ff'' = \frac{1}{2}\left[f'^2 - \theta\right] \tag{3.51}$$

(b) ϕ equation

$$\phi'' + f\mathrm{Sc}\phi' = 0 \tag{4.11}$$

(c) Fuel mass fraction equation

$$\frac{1}{\mathrm{Sc}} Y_F'' + fY_F' = \frac{D_1 \nu_F M_F Y_O Y_F e^{-E^*/\theta}}{\theta} \tag{3.62}$$

The relation between Y_F and θ was given by equation (4.22) and between Y_F and Y_O by equation (4.24)

The boundary conditions are

at $\eta = 0$:

$f'(0) = 0$

$f(0) = \bar{f}_w$ } given

$\phi(0) = 1$

$f''(0)$

$\phi'(0)$ } unknown

$Y_{F,w}$

at $\eta \to \infty$:

$f'(\infty) = 1$

$\phi(\infty) = 0$

$Y_F(\infty) = 0$

where $Y_{F,w}$ and $Y'_{F,w}$ relate to each other by equation (3.67a).

4.5 Numerical Method

Because of the compressible flow, equation (3.51) is temperature dependent and hence the conservation equations must be solved simultaneously. The unknown conditions must be assumed to reduce the problem to an initial value problem for which the Adams-Moulton integration method can be applied. After the trial solutions are obtained the known boundary conditions at the edge of the integration interval are compared with the correspondent values provided by the trial solutions. If the solutions at this point do not agree with the known values another guess must be used and the integration is repeated. This procedure continues until the solutions provided by the initial guess conditions converge to the known conditions at the edge of the boundary layer.

In order to reduce the guess work and computer time the corrections are made for the initial guess by the Newton-Raphson Method. In so doing a number of additional differential equations are required and have to be integrated. These equations are obtained by differentiating the terms of the initial differential equations with respect to the initial guess conditions. The integrals of these equations, henceforth referred to as perturbation equations, give the rate of change of the integrals of the original differential equations with respect to initial conditions. The following procedures are illustrated for the iterative procedure described above.

The unknown boundary conditions are

$$\left.\begin{aligned} f''(0) &= X \\ \phi'(0) &= Y \\ Y_{F,w} &= Z \end{aligned}\right\} \qquad (4.31a)$$

The problem is to find the value of X, Y and Z to be such that the boundary conditions at the edge are satisfied, that is, it is desirable to find a solution of

$$\left.\begin{aligned} f'(\infty)[X,Y,Z] &= 1 \\ \phi(\infty)[X,Y,Z] &= 0 \\ Y_F(\infty)[X,Y,Z] &= 0 \end{aligned}\right\} \qquad (4.31b)$$

Therefore, the necessary correction to the first approximation by using the Newton-Raphson method comes from the solution of the following set of equations:

$$\left.\begin{aligned} 1 &= f' + \frac{\partial f'}{\partial X}\Delta X + \frac{\partial f'}{\partial Y}\Delta Y + \frac{\partial f'}{\partial Z}\Delta Z \\ 0 &= \phi + \frac{\partial \phi}{\partial X}\Delta X + \frac{\partial \phi}{\partial Y}\Delta Y + \frac{\partial \phi}{\partial Z}\Delta Z \\ 0 &= Y_F + \frac{\partial Y_F}{\partial X}\Delta X + \frac{\partial Y_F}{\partial Y}\Delta Y + \frac{\partial Y_F}{\partial Z}\Delta Z \\ 0 &= f'' + \frac{\partial f''}{\partial X}\Delta X + \frac{\partial f''}{\partial Y}\Delta Y + \frac{\partial f''}{\partial Z}\Delta Z \\ 0 &= \phi' + \frac{\partial \phi'}{\partial X}\Delta X + \frac{\partial \phi'}{\partial Y}\Delta Y + \frac{\partial \phi'}{\partial Z}\Delta Z \\ 0 &= Y_F' + \frac{\partial Y_F'}{\partial X}\Delta X + \frac{\partial Y_F'}{\partial Y}\Delta Y + \frac{\partial Y_F'}{\partial Z}\Delta Z \end{aligned}\right\} \qquad (4.32)$$

where ΔX, ΔY and ΔZ are corrections for X, Y and Z, respectively. Let

$$\delta_1 = f' + f'_X\Delta X + f'_Y\Delta Y + f'_Z\Delta Z - 1$$

$$\delta_2 = \phi + \phi_X\Delta X + \phi_Y\Delta Y + \phi_Z\Delta Z$$

$$\delta_3 = Y_F + Y_{FX}\Delta X + Y_{FY}\Delta Y + Y_{FZ}\Delta Z$$

$$\delta_4 = f'' + f''_X\Delta X + f''_Y\Delta Y + f''_Z\Delta Z$$

$$\delta_5 = \phi' + \phi'_X\Delta X + \phi'_Y\Delta Y + \phi'_Z\Delta Z$$

$$\delta_6 = Y'_F + Y'_{FX}\Delta X + Y'_{FY}\Delta Y + Y'_{FZ}\Delta Z$$

where subscripts X, Y, Z indicate partial derivative respect to X, Y and Z.

Value of ΔX, ΔY, ΔZ should be such that $(\delta_1^2 + \delta_2^2 + \delta_3^2 + \delta_4^2 + \delta_5^2 + \delta_6^2)$ is minimum. To minimize the sum, it is necessary to equate its derivative with respect to ΔX, ΔY, ΔZ to zero and this calculation yields a value of ΔX, ΔY, ΔZ corresponding to the minimum of the sum from the following matrix

$$\begin{bmatrix} a(1,1) & a(1,2) & a(1,3) \\ a(2,1) & a(2,2) & a(2,3) \\ a(3,1) & a(3,2) & a(3,3) \end{bmatrix} \begin{bmatrix} \Delta X \\ \Delta Y \\ \Delta Z \end{bmatrix} = \begin{bmatrix} a(1,4) \\ a(2,4) \\ a(3,4) \end{bmatrix} \quad (4.34)$$

where

$$a(1,1) = f_X'^2 + \phi_x^2 + Y_{FX}^2 + f_X''^2 + \phi_X'^2 + Y_{FX}'^2$$

$$a(1,2) = f_X'f_Y' + \phi_X\phi_Y + Y_{FX}Y_{FY} + f_X''f_Y'' + \phi_X'\phi_Y' + Y_{FX}'Y_{FY}'$$

$$a(1,3) = f_X'f_Z' + \phi_X\phi_Z + Y_{FX}Y_{FZ} + f_X''f_Z'' + \phi_X'\phi_Z' + Y_{FX}'Y_{FZ}'$$

$$a(1,4) = f_X' - f'f_X' - \phi\phi_X - Y_FY_{FX} - f''f_X'' - \phi'\phi_X' - Y_F'Y_{FX}'$$

$$a(2,1) = a(1,2)$$

$$a(2,2) = f_Y'^2 + \phi_Y^2 + Y_{FY}^2 + f_Y''^2 + \phi_Y'^2 + Y_{FY}'^2$$

$$a(2,3) = f_Y'f_Z' + \phi_Y\phi_Z + Y_{FY}Y_{FZ} + f_Y''f_Z'' + \phi_Y'\phi_Z' + Y_{FY}'Y_{FZ}'$$

$$a(2,4) = f_Y' - f'f_Y' - \phi\phi_Y - Y_FY_{FY} - f''f_Y'' - \phi'\phi_Y' - Y_F'Y_{FY}'$$

$$a(3,1) = a(1,3)$$

$$a(3,2) = a(2,3)$$

$$a(3,3) = f_Z'^2 + \phi_Z^2 + Y_{FZ}^2 + f_Z''^2 + \phi_Z'^2 + Y_{FZ}'^2$$

$$a(3,4) = f_Z' - f'f_Z' - \phi\phi_Z - Y_FY_{FZ} - f''f_Z'' - \phi'\phi_Z' - Y_F'Y_{FZ}'$$

value of a(1,1)...a(3,4) can be obtained after the partial derivatives are calculated at η_{edge}. These partial derivatives come from differentiation of the original differential equations with respect to X, Y and Z.

The following is only the perturbation equations for the momentum equation presented as an example.

$$\left.\begin{aligned} f_X''' &= -(f_X f'' + f_X'' f) + \tfrac{1}{2}(2f' f_X' - \theta_X) \\ f_Y''' &= -(f_Y f'' + f_Y'' f) + \tfrac{1}{2}(2f' f_Y' - \theta_Y) \\ f_Z''' &= -(f_Z f'' + f_Z'' f) + \tfrac{1}{2}(2f' f_Z' - \theta_Z) \end{aligned}\right\} (4.35)$$

Similarly the partial derivatives for ϕ and Y_F can be obtained.

These perturbation equations are integrated with the initial conditions.

$$\left.\begin{aligned} \eta = 0: \quad & f_X = f_X' = Y_{FX} = \phi_X = \phi_X' = Y_{FX}' = 0 \\ & f_Y = f_Y' = Y_{FY} = \phi_Y = \phi_Y'' = Y_{FY}' = 0 \\ & f_Z = f_Z' = f_Z'' = \phi_Z = Y_{FZ}' = \phi_Z' = 0 \\ & f_X'' = \phi_Y' = Y_{FZ} = 1 \end{aligned}\right\} (4.36)$$

Additional details can be found in Reference [26].

The above iterative procedure was used to integrate the set of conservation equations for various D_1, θ_w and $\bar{f}_w$ values. In order to approximate the first estimates, the assumption of incompressible flow is important for decoupling the momentum equation from the energy equation. The solutions provided by the incompressible solutions, then were used as the first approximation for the compressible case with the same D_1 value. For the new D_1 value the previous solutions were used as the initial guess.

CHAPTER V

RESULTS AND DISCUSSION

5.1 Introduction

This chapter deals with numerical results achieved through the iterative procedures described in the previous chapter.

Two types of solution were obtained, dependent on either the injection rate or the wall temperature. The effect of these independent parameters on the surface heat transfer rate and the fuel mass fraction at the wall have been investigated using various plots. These are presented and discussed in the sections which follow. Additional results have been included in the Appendix. Temperature and fuel mass fraction profiles have also been established. Finally, to complete this chapter a plot of $f''(0)$ versus D_1 is given from which the skin friction can be calculated.

5.2 Numerical Constants and Range of Parameters

The calculations on the physical problem discussed thus far were carried out using the following data for methane and air at 1 atm and $T_e = 300°K$

$$q° = 191.579 \text{ kcal/g-mole of } CH_4$$

$$\rho_e = 0.0013 \text{ g/cm}^3$$

$$C_{p,e} = 0.341 \text{ cal/g-°K}$$
$$Y_{O,e} = 0.232$$
$$E = 77.454 \text{ kcal/g-mole}$$

In order to investigate the effects of injection rate, the injection parameter $\bar{f}_w$ was taken to be -0.02, -0.03, and -0.05. The effects of wall temperature were also examined by taking the dimensionless temperature at the wall θ_w to be 2.5, 3.0, and 4.5.

5.3 Numerical Results and Discussion

5.3.1 Effects of Injection Rate

From the numerical solutions the main results relate the independent parameters the First Damkohler Number D_1, the wall temperature θ_w, and the fuel injection rate $\bar{f}_w$ to the surface heat transfer and the fuel concentration at the wall. These results are displayed in Figures 3, 4, 5, and 6.

The values of the surface heat transfer $Nu/(Re)^{1/2}$ as a function of the First Damkohler Number D_1 with the fuel injection rate $\bar{f}_w$ as a parameter are shown in Figure 3. The wall temperature θ_w has been fixed at value of 3.0. These establish two types of transition which depend on the values of $\bar{f}_w$. The simple transition solutions were obtained for $\bar{f}_w$ = -0.02 and -0.03 where the values of $Nu/(Re)^{1/2}$ increase with increasing D_1. Higher value of $\bar{f}_w$ gives still higher values of $Nu/(Re)^{1/2}$, making the slopes of the curves

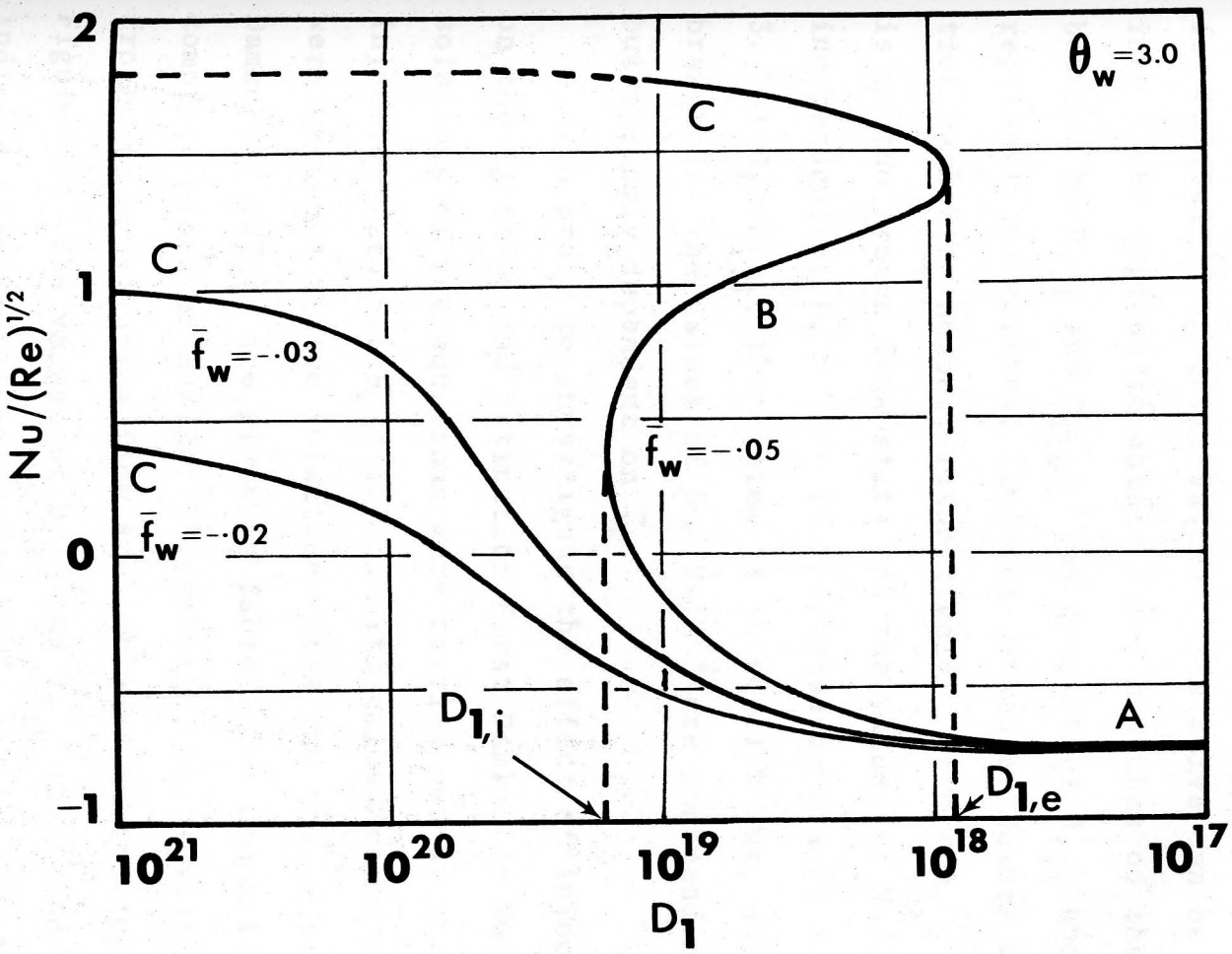

Figure 3. Effect of Injection Rate on Surface Heat Transfer, $\theta_w = 3.0$

to increase.

At a fuel injection rate of $\bar{F}_w = -0.05$, the solution for $Nu/(Re)^{1/2}$ is multi-valued. The curve can be divided into three regions to obtain three branches of the solution bounded by $D_{1,i}$ and $D_{1,e}$. The quantities $D_{1,i}$ and $D_{1,e}$ represent the critical Ignition Damkohler Number and Extinction Damkohler Number, respectively. At $D_1 << D_{1,e}$ the system is in the frozen flow state and the values of $Nu/(Re)^{1/2}$ are independent of D_1. This is indicated as branch A on Figure 3. At $D_1 >> D_{1,i}$, the system is in equilibrium, shown as branch C. The values of $Nu/(Re)^{1/2}$ are independent of D_1 but strongly dependent on $\bar{F}_w$.

In order to investigate the effect of injection rate on the Ignition and Extinction First Damkohler Numbers solutions of the equations were carried out at three injection rates at $\theta_w = 2.5$. Multi-valued transition curves were obtained at two injection rates and the critical Damkohler values are given in Table 1 for comparison. The complete plots of $Nu/(Re)^{1/2}$ versus D_1 encompassing from frozen to equilibrium flow are included in the Appendix in Figure A1. The values of $D_{1,i}$ and $D_{1,e}$ tabulated in Table 1 indicate that the higher value of $\bar{F}_w$ requires smaller values of the critcal First Damkohler Numbers. Surface heat transfer results at $\theta_w = 4.5$ are also included in the Appendix in Figure A3.

The effects of the injection rate on fuel concentration

Table 1. Effect of Injection Rate on Ignition and Extinction Damkohler Numbers at $\theta_w = 2.5$

$\bar{f}_w$	$D_{1,i}$	$D_{1,e}$
-0.03	10^{23}	3×10^{22}
-0.05	4.3×10^{22}	9.1×10^{18}

at the wall are shown in Figure 4. The dimensionless fuel mass fraction at the wall $\alpha_{F,w}$ as a function of the First Damkohler Number D_1 is presented with $\bar{f}_w$ as a parameter. In Table 2, the limiting values of the fuel mass fraction at the wall under frozen flow condition, $(Y_{F,w})_f$ are tabulated for $\theta_w = 3.0$ at different $\bar{f}_w$. The results show that the fuel mass consumption at the wall for small $\bar{f}_w$ (i.e. $\bar{f}_w$ = -0.02 and -0.03) is very small and increases drastically when D_1 increases. This physical situation leads to prediction that the reaction will occur right at the surface with fuel concentrations going to zero and oxygen concentrations establishing finite values. Therefore the reaction is not strong and the T_{max} is lower than that required for multi-transition from frozen to equilibrium flow. The simple transition, therefore, tends to exist.

At higher values of $\bar{f}_w$, say -0.05, these values are rather high. The reaction zone moves into the boundary layer towards the point where fuel and oxygen mixes together

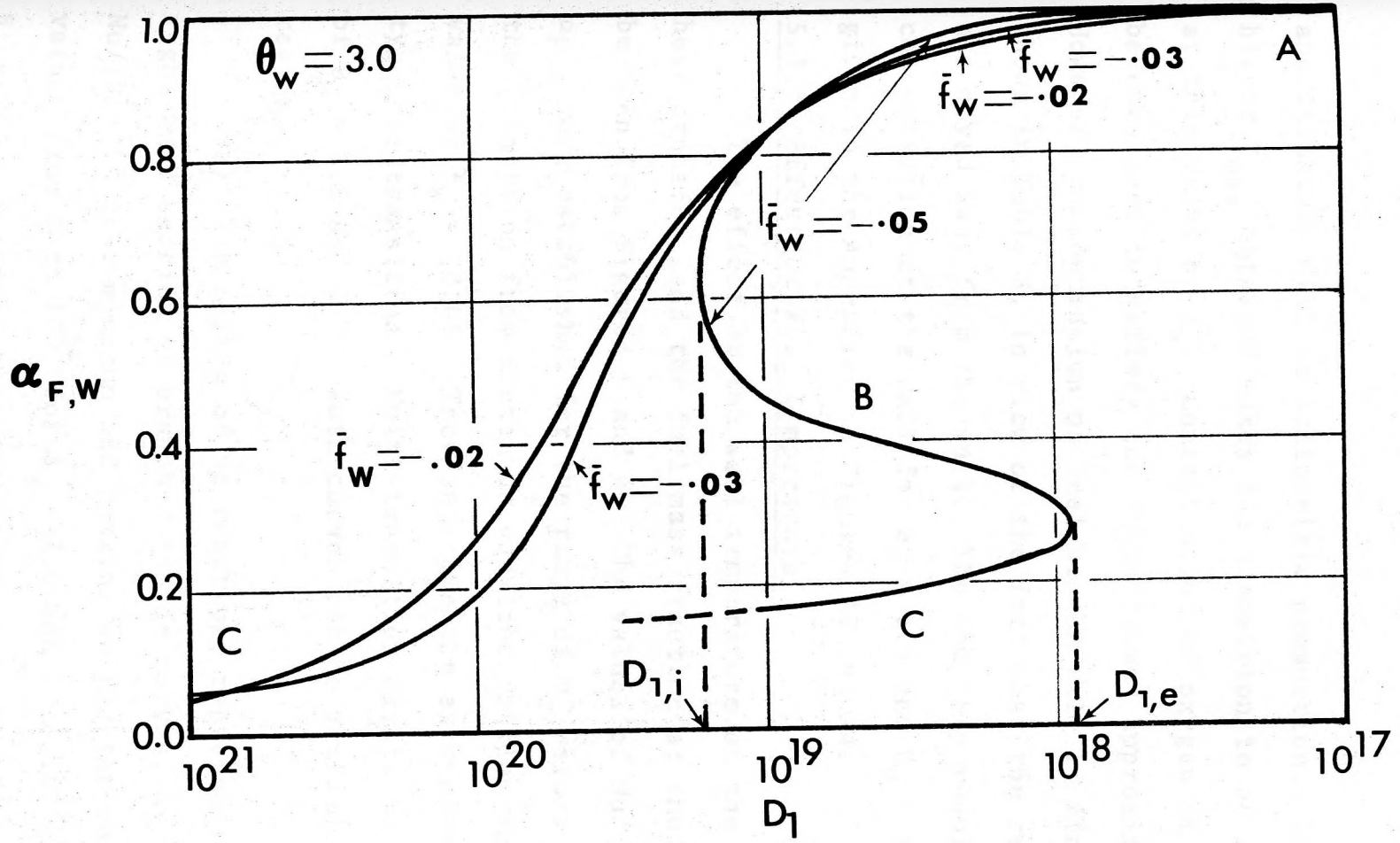

Figure 4. Effect of Injection Rate on Fuel Mass Fraction at the Wall, θ_w = 3.0

approximately with stoichiometric proportion. Therefore the higher T_{max} obtained makes the transition to be multi-valued at this value of θ_w. Concentration of oxygen at the wall becomes zero to satisfy the "thin flame" approximation. However, concentration of fuel at the wall is finite, as shown in Table 3, in view of the fact that the reaction zone has moved away from the wall. The complete results of fuel concentration at the wall for $\theta_w = 2.5$ and $\theta_w = 4.5$ are given in the Appendix, in Figures A2 and A4.

5.3.2 Effect of Wall Temperature

The effect of the wall temperature on the surface heat transfer and the fuel mass fraction at the wall can be seen from Figures 5 and 6. The values of $Nu/(Re)^{1/2}$ and $\alpha_{F,w}$ were established for the range of D_1 values encompassing the transition from frozen to equilibrium flow and for fixed value of $\bar{f}_w = -0.05$. They indicate the existence of two types of transition. Multi-transition exists for the values of $\theta_w = 2.5$ and 3.0. Both curves can be divided into three regions.

(a) The region of no reaction, representing the right-hand section of branch A on the curves, is where $Nu/(Re)^{1/2}$ is a minimum and remains so for the range of D_1 values from 0 to 10^{16} for $\theta_w = 3.0$ and 0 to 10^{19} for $\theta_w = 2.5$. No combustion can be observed in this region and values of $Nu/(Re)^{1/2}$ as well as of $\alpha_{F,w}$ are independent of D_1 but vary slightly with θ_w. This is in agreement with the

Table 2. Comparison of $(Y_{F,w})_f$ with Different $\bar{f}_w$, $\theta_w = 3.0$

$\bar{f}_w$	-0.02	-0.03	-0.05
$(Y_{F,w})_f$	0.02723	0.04063	0.06700

Table 3. Effects of Injection Rate on $(Y_{F,w})_{equil}$ and $(Y_{O,w})_{equil}$, $\theta_w = 2.5$

$\bar{f}_w$	$(Y_{F,w})_{equil}$	$(Y_{O,w})_{equil}$
-0.02	0	0.11504
-0.03	0	0.05976
-0.05	0.01074	0

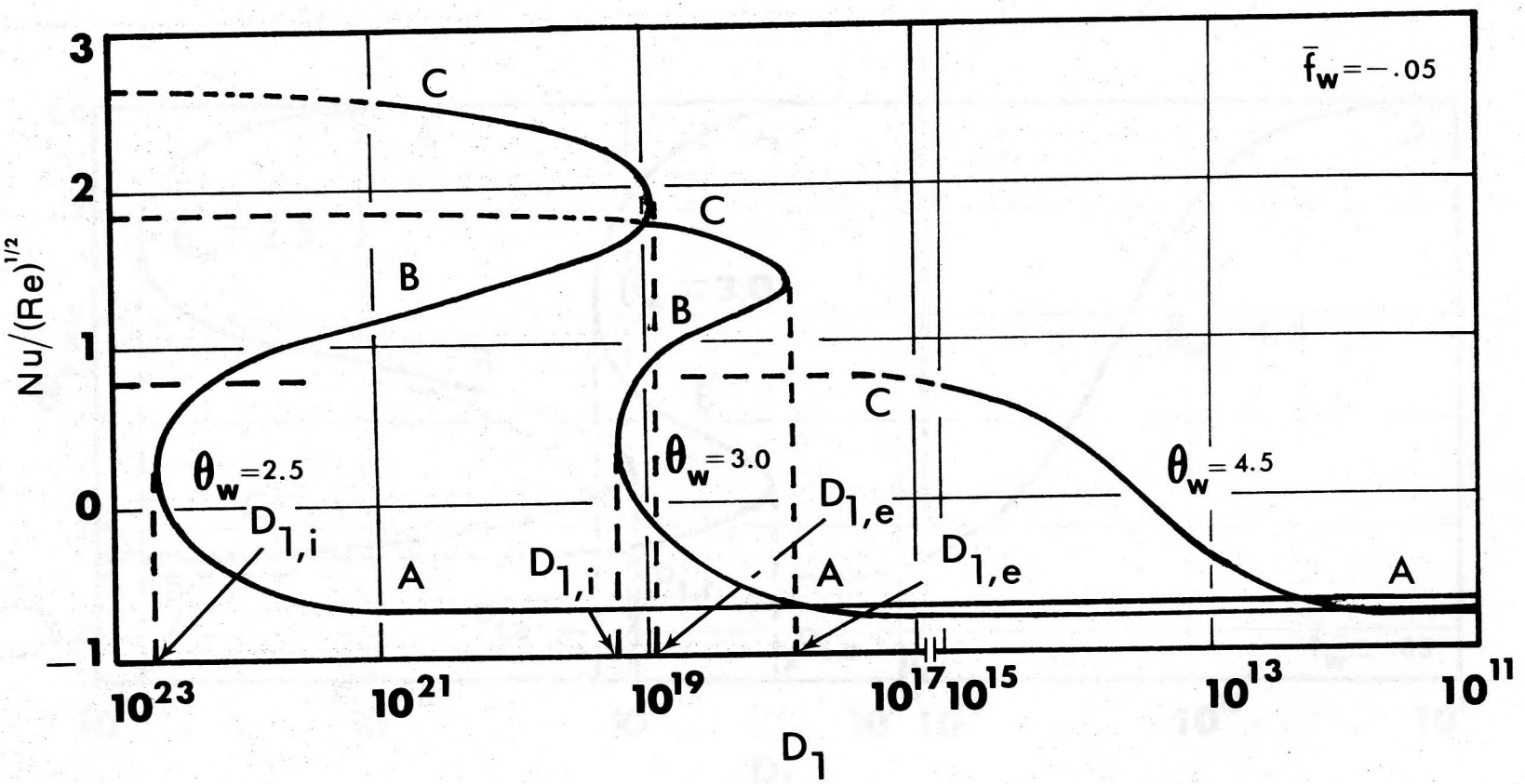

Figure 5. Effect of Wall Temperature on Surface Heat Transfer, $\bar{f}_w$ = -0.05

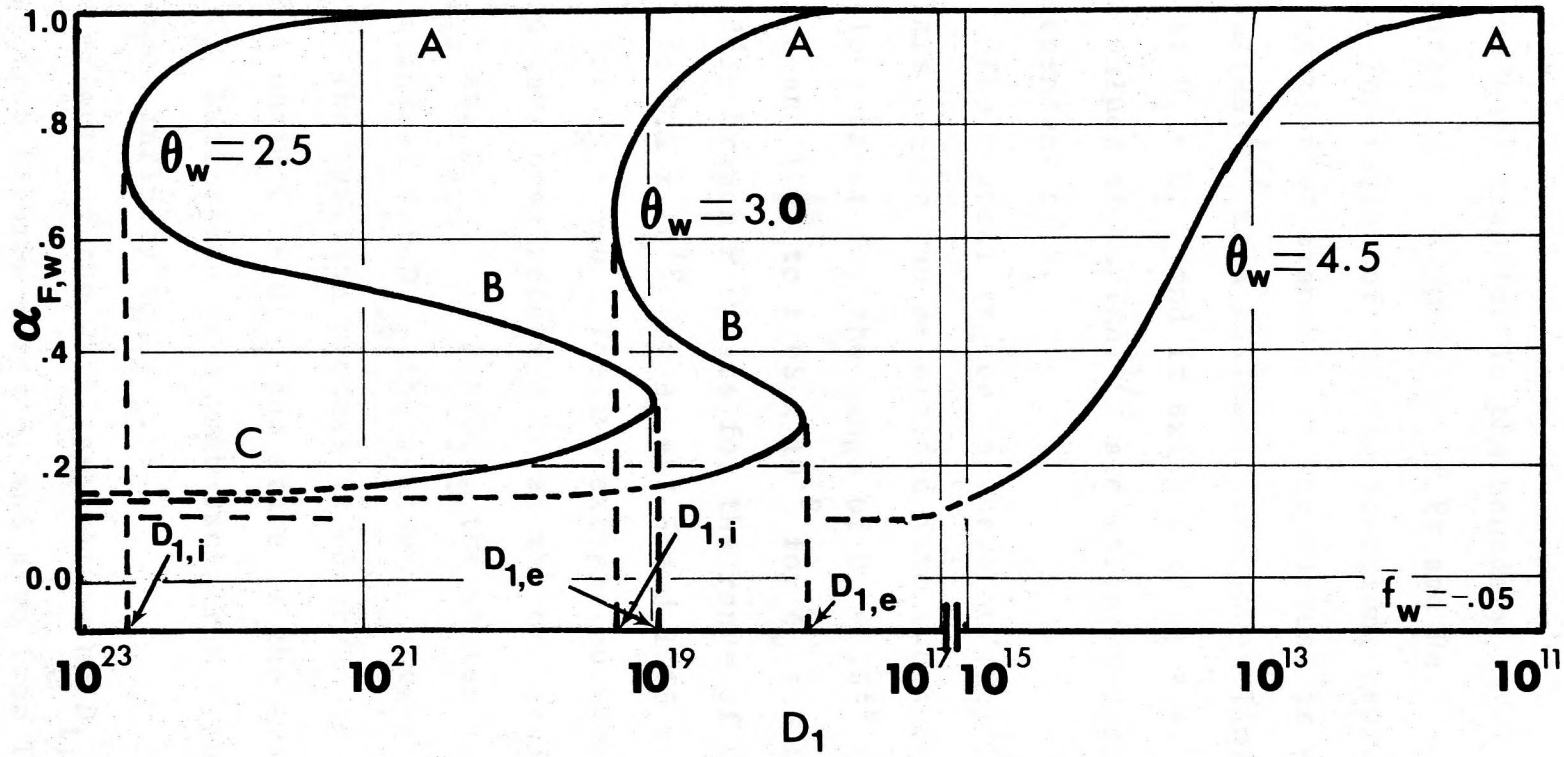

Figure 6. Effect of Wall Temperature on Fuel Mass Fraction at the Wall, $\bar{f}_w = -0.05$

non-reactive heat transfer in the boundary layer by which Nu was determined to be a function of Pr and Re.

(b) The region of intense reaction, representing the left-hand section of branch C on the curves, is where the value of $Nu/(Re)^{1/2}$ is a maximum. The lower limit of this region is at $D_1 = D_{1,e}$ and it extends to $D_1 = \infty$. In this region the values of $Nu/(Re)^{1/2}$ are strongly dependent on θ_w and independent of D_1.

(c) The central region is where $Nu/(Re)^{1/2}$ is multi-valued. This region can be divided into two subregions. Weak reactions exist for the range of $D_1 = 10^{19}$ to 4.3×10^{22} for $\theta_w = 2.5$ and 10^{16} to 1.65×10^{19} for $\theta_w = 3.0$ on branch A. The middle branch B exists for the range of D_1 from 4.3×10^{22} to 9.1×10^{18} for $\theta_w = 2.5$ and 1.65×10^{19} to 8.7×10^{17} for $\theta_w = 3.0$. The two extreme boundaries for this region have been referred to as the critical Damkohler Numbers $D_{1,i}$ and $D_{1,e}$. If $D_1 >> D_{1,i}$ the system is always in equilibrium and if $D_1 << D_{1,e}$ the system is always in frozen flow state. The ignition process is observed as D_1 increases for branch A until $D_1 = D_{1,i}$ the state of the system jumps to branch C. Extinction is a jump back from C to A when D_1 decreases from infinity to $D_{1,e}$.

The effects of the wall temperature on $D_{1,i}$ and $D_{1,e}$ can be seen from Figures 5 and 6, and also from Table 4. When θ_w increases, both $D_{1,i}$ and $D_{1,e}$ decrease and the range of D_1 for which three branch solutions exist also

Table 4. Dependence of Critical Damkohler Numbers on θ_w, $\bar{f}_w = -0.05$

θ_w	$D_{1,i}$	$D_{1,e}$
2.5	4.3×10^{22}	9.1×10^{18}
3.0	1.65×10^{19}	8.7×10^{17}

decreases. This leads to a simple transition flow at higher value of θ_w as it is the case for $\theta_w = 4.5$. This state is called the no-extinction state.

Comparisons of the surface heat transfer rates at the three wall temperatures for a fuel injection rate $\bar{f}_w$ of -0.02 and -0.03 are given in the Appendix, Figures A5 and A7.

The effects of wall temperature on the fuel concentration at the wall are displayed in Figure 6, and summarized in Table 5. The curves in Figure 6 are similar to those in Figure 5. That is the multi-valued transition occurs when $\theta_w = 2.5$ and 3.0 but only a simple transition at $\theta_w = 4.5$. In the frozen flow region the values of $\alpha_{F,w}$ are unity and the values of $(Y_{F,w})_f$ are independent of D_1 but dependent of θ_w, as shown in Table 5. The higher values of θ_w provide a lower value of $(Y_{F,w})_f$. The maximum value of D_1 for the system to be in frozen flow depends on θ_w whereby the higher values of θ_w require allower value of D_1 for the system to be in frozen flow.

Table 5. Comparison of $(Y_{F,w})_f$ and $(Y_{F,w})_{equil}$ for Different θ_w, $\bar{f}_w = -0.05$

θ_w	2.5	3.0	4.5
$(Y_{F,w})_f$	0.06856	0.06700	0.06328
$(Y_{F,w})_{equil}$	0.01074	0.009719	0.00743

Comparisons of the fuel concentrations at the wall at the three wall temperatures for a fuel injection rate $\bar{f}_w$ of -0.02 and -0.03 are given in the Appendix, Figures A6 and A8.

5.3.3 The Profiles

The temperature distributions in the reactive boundary layer (taken at $\bar{f}_w = -0.05$ and $\theta_w = 2.5$) are shown in Figure 7. For branch A the T_{max} is at the wall while for branch B the T_{max} exists somewhere close to the surface and indicates the flame location. When D_1 increases the reaction zone moves towards the wall. On branch C the peak of these curves also moves towards the wall as the First Damkohler increases. The maximum temperature is almost constant and independent of the First Damkohler Number.

The effect of θ_w on the temperature profiles can be seen from Figure 8. For the same value of D_1, the reaction zone is closer to the surface for the higher value of θ_w and T_{max} is lower than θ_w is higher. The effects of the fuel

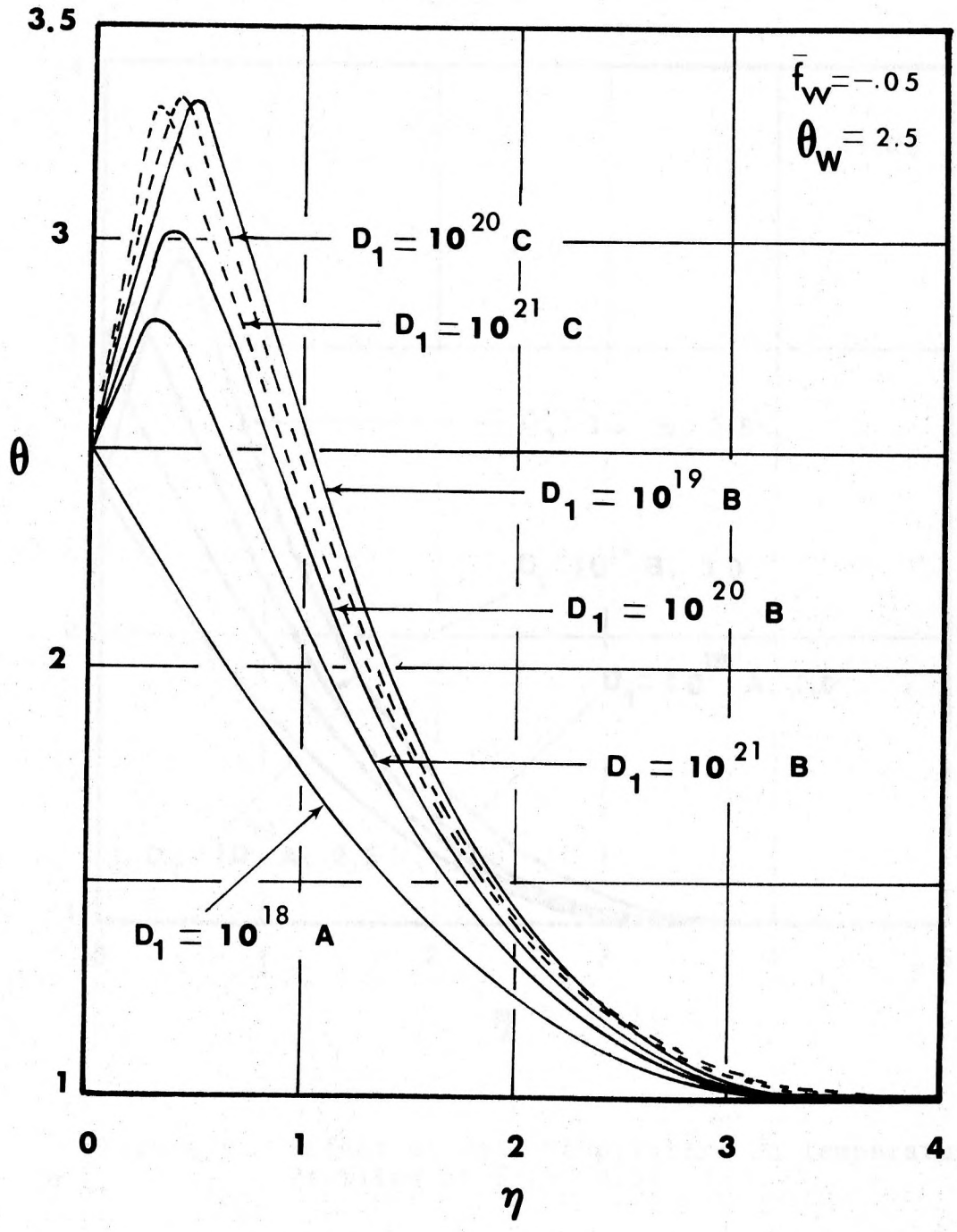

Figure 7. Temperature Profiles at θ_w = 2.5 and $\bar{f}_w$ = -0105

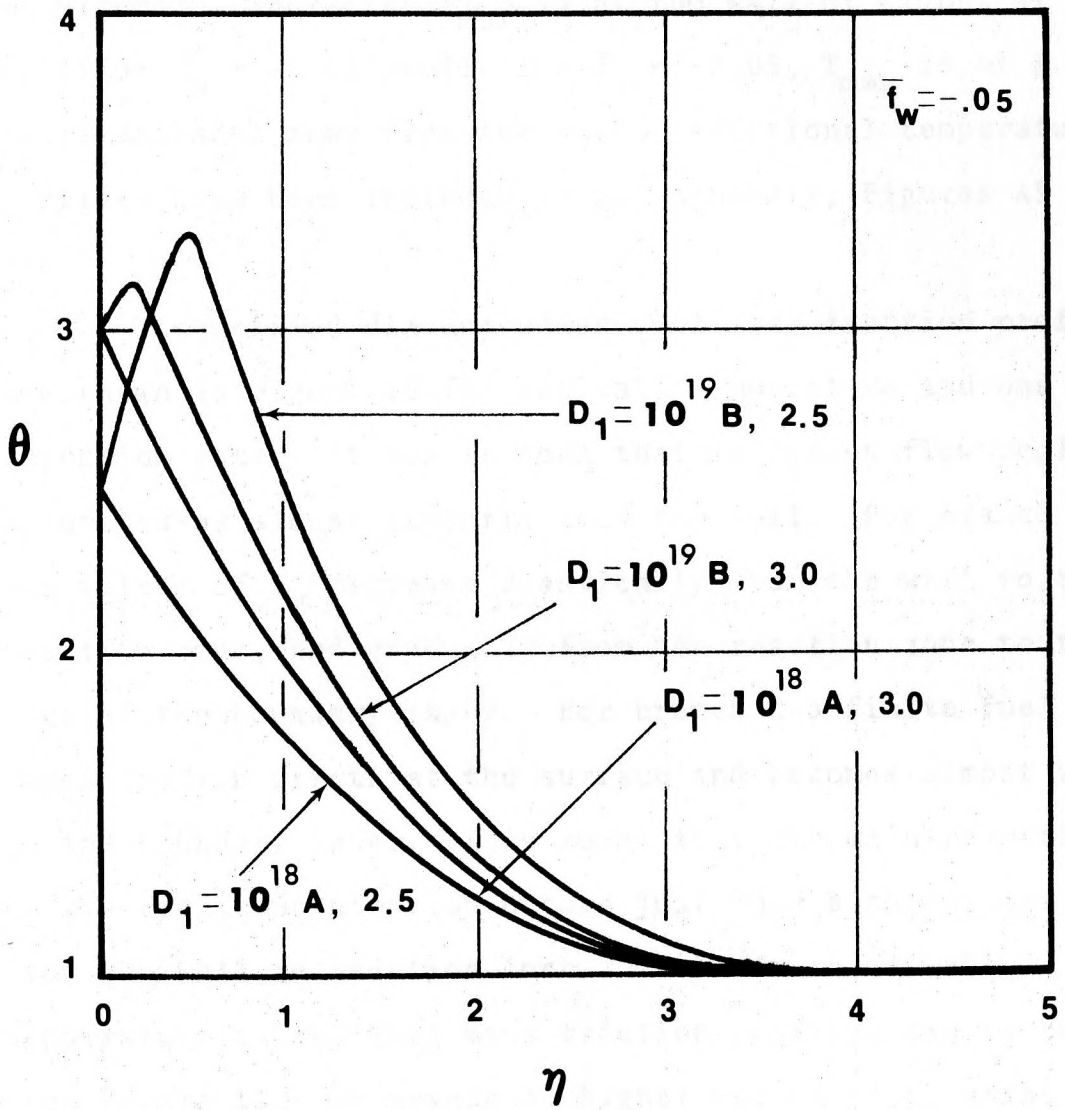

Figure 8. Effect of Wall Temperature on Temperature Profiles at $\bar{f}_w = -0.05$

injection rate on the temperature profile are displayed in Figure 9, where the T_{max} is at the wall or almost at the wall for $\bar{f}_w = -0.02$ while for $\bar{f}_w = -0.05$, T_{max} is at a short distance away from the wall. Additional temperature profiles have been included in the Appendix, Figures A9 and A10.

The defined dimensionless fuel mass fraction profiles are shown in Figure 10 for one wall temperature and one injection rate. It can be seen that in frozen flow region α_F decreases almost linearly from the wall. For branch B the values of α_F decrease drastically from the wall to the reaction zone, and gradually from the reaction zone to the edge of the boundary layer. For branch C a finite fuel concentration exists at the surface and becomes almost zero in the boundary layer. This means that the main reduction in the fuel concentration occurs just only a short distance from the wall to reaction zone. The effects of wall temperature on the fuel mass fraction profiles can be seen from Figure 11. On branch A, higher values of α_F exist for the low θ_w while on branch B the lower values of α_F occur at the low θ_w. Additional fuel concentration profiles are included in the Appendix, Figures A11-A18.

Velocity distribution are also shown in Figure 13 for $\bar{f}_w = -0.05$ and $\theta_w = 2.5$. A plot of $f''(0)$ as a function of D_1 is given in Figure 14 for two wall temperatures. The effects of chemical kinetics on the skin friction can be

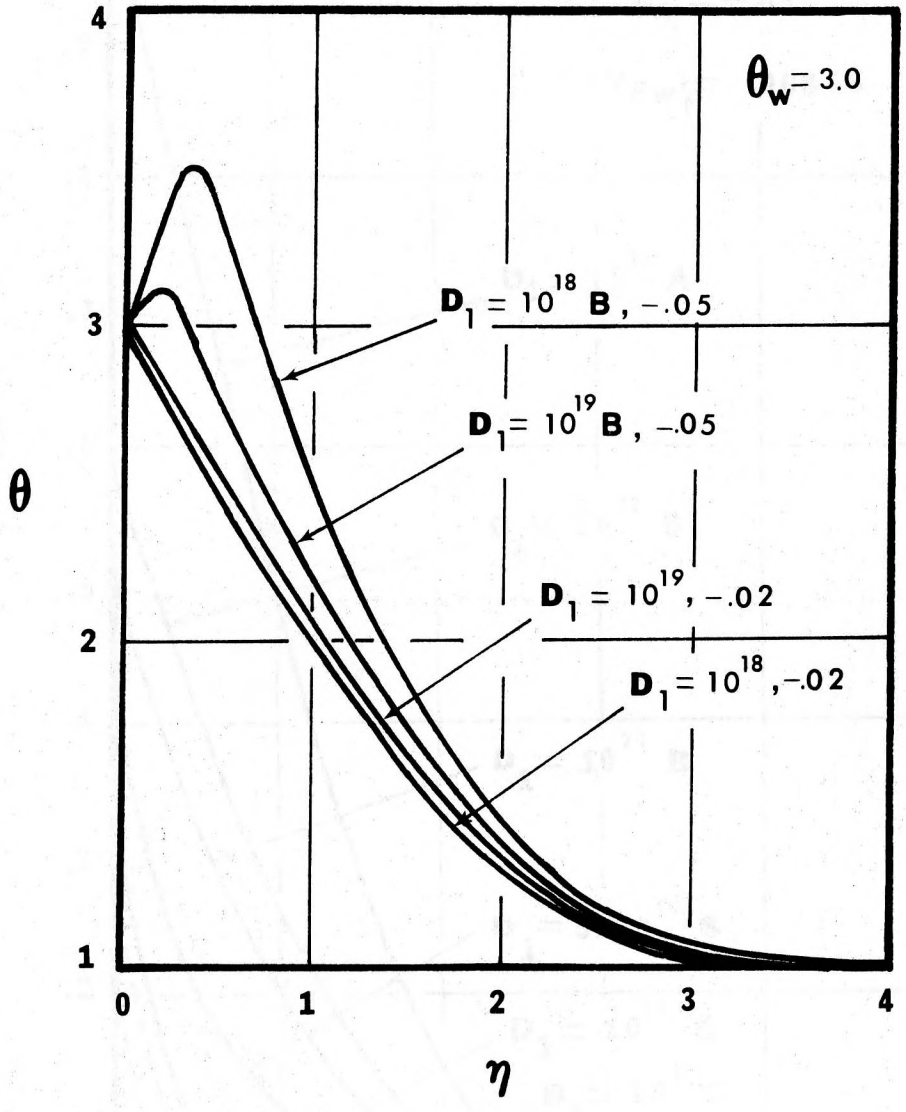

Figure 9. Effect of Injection Rate on Temperature Profiles at $\theta_w = 3.0$

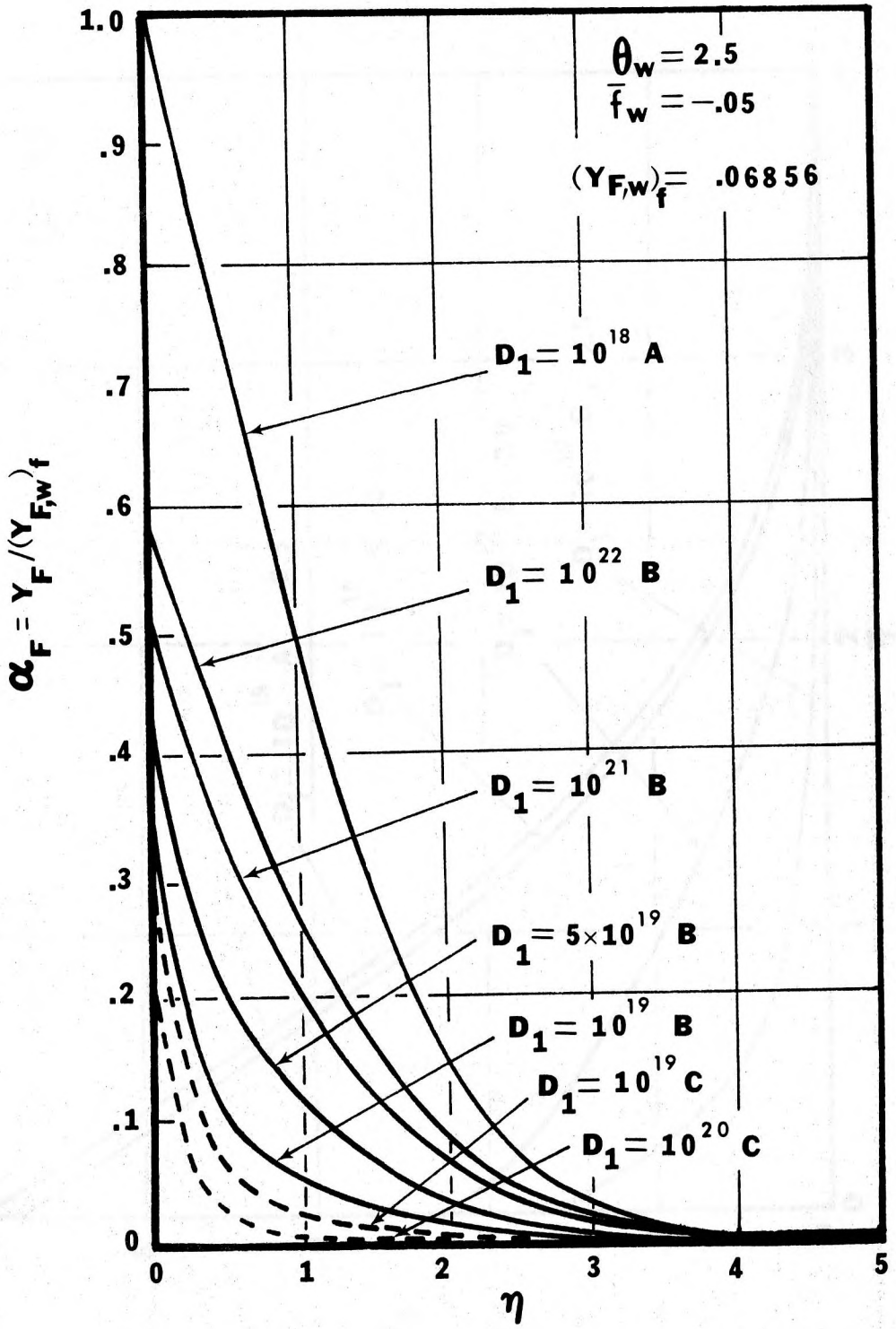

Figure 10. Fuel Mass Fraction Profiles at $\theta_w = 2.5$ and $\bar{f}_w = -0.05$

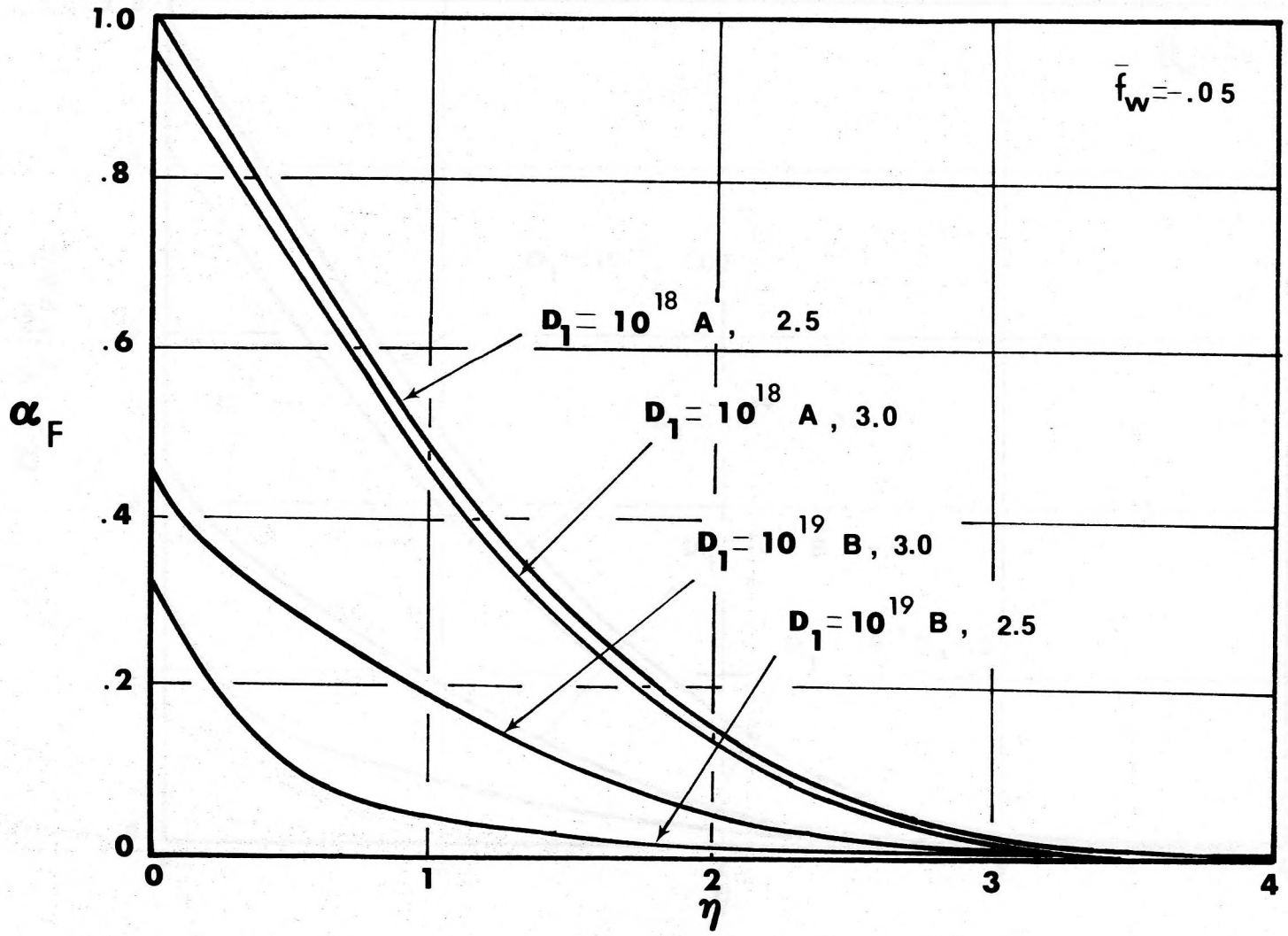

Figure 11. Effect of Wall Temperature on Fuel Mass Fraction Profiles at $\bar{f}_w$ = -0.05

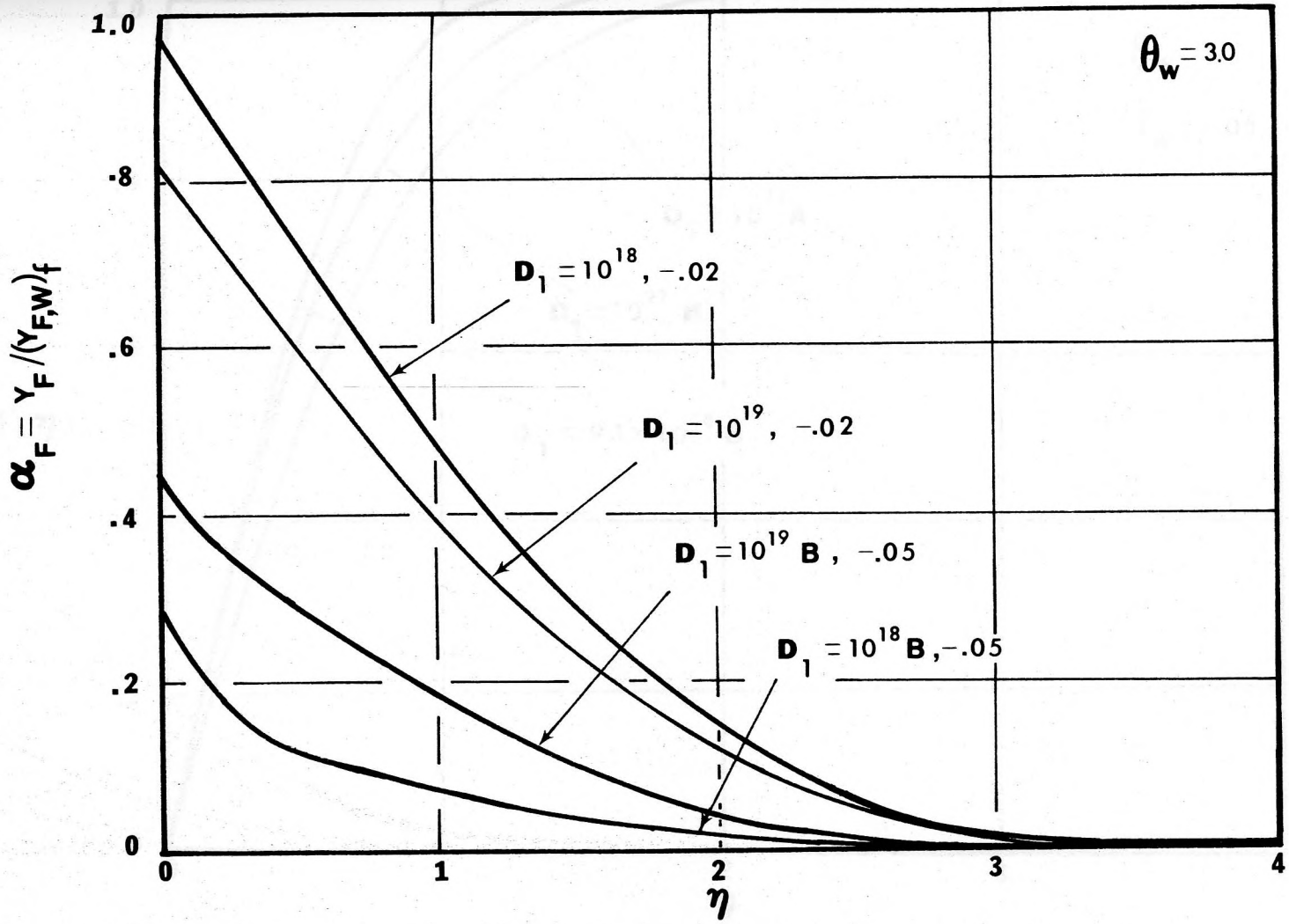

Figure 12. Effect of Injection Rate on Fuel Mass Fraction Profiles at $\theta_w = 3.0$

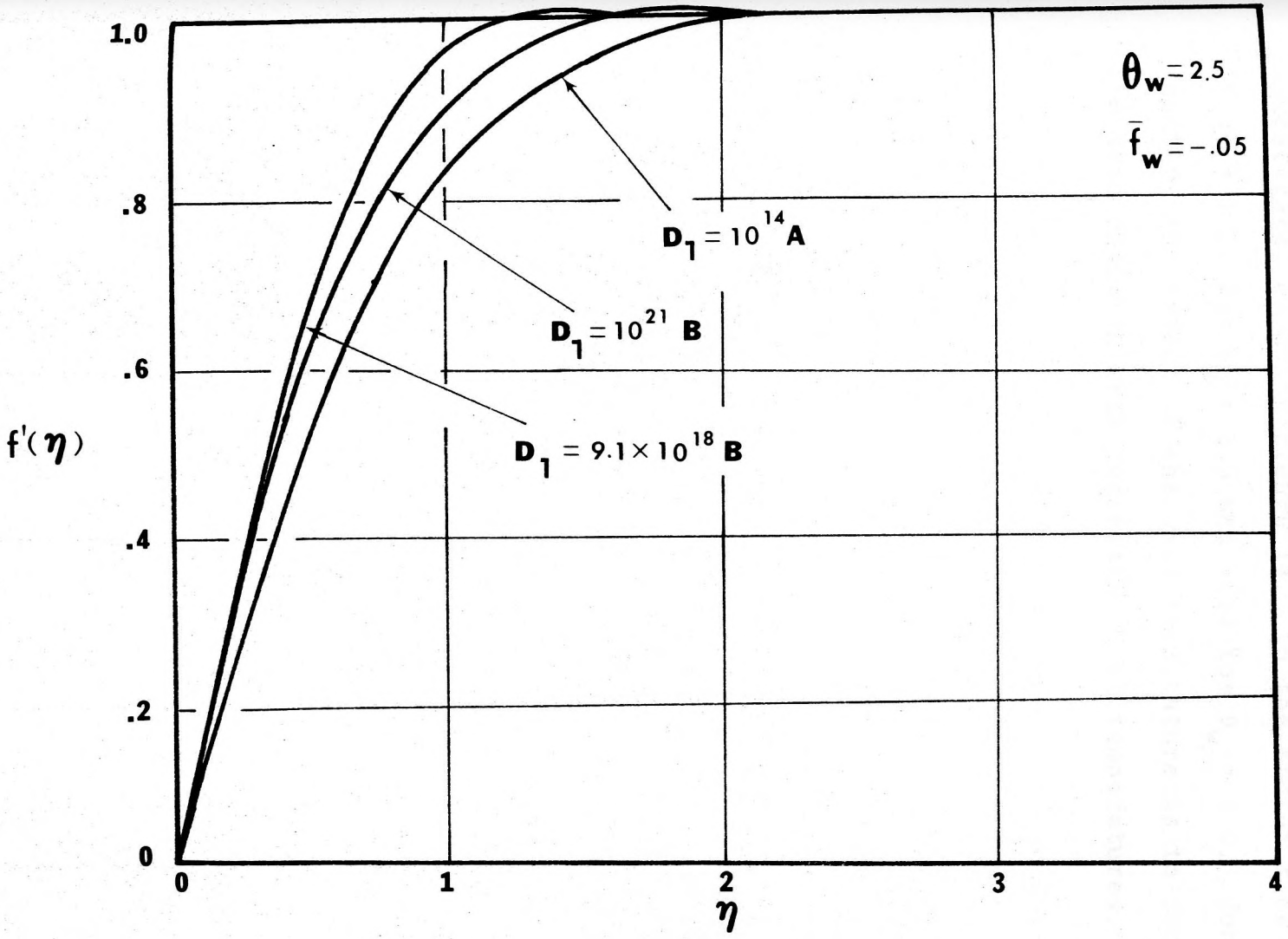

Figure 13. Velocity Profiles at θ_w = 2.5 and $\bar{f}_w$ = -0.05

investigated by using Figure 14. In the frozen flow region $f''(0) = 1.37$ for $\theta_w = 2.5$ and 1.52 for $\theta_w = 3.0$. Consequently, the effect of the wall temperature is to increase the skin friction with increasing wall temperatures.

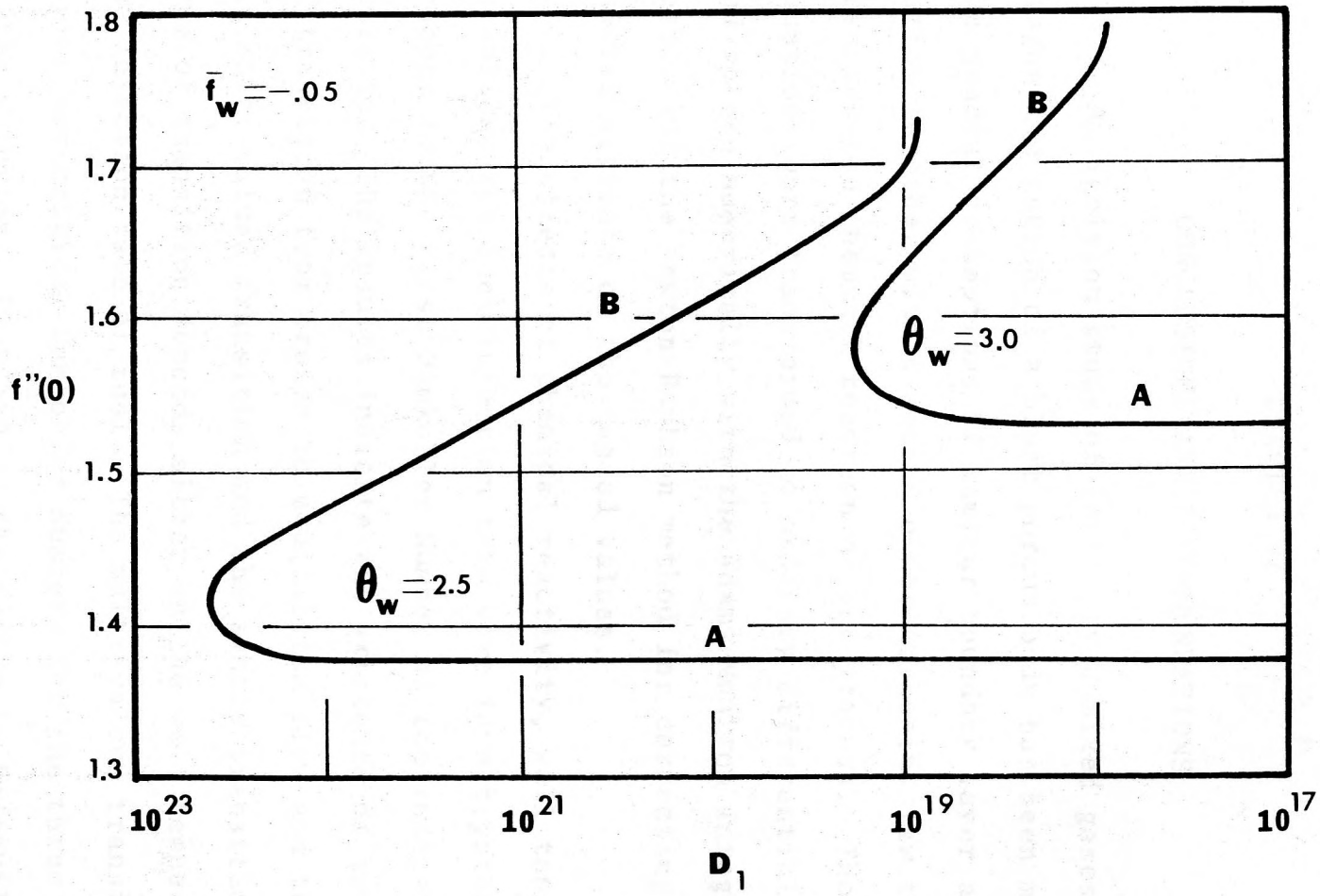

Figure 14. Plot of f"(0) Versus D_1

CHAPTER VI

CONCLUSIONS AND RECOMMENDATIONS

An ignition study of initially unmixed gases at stagnation region of a blunt porous body has been made with the general assumptions of laminar boundary layer approximation together with a second order Arrhenius law to describe the chemical reaction of the process. The general equations were transformed to ordinary differential equations and solved numerically with the Adams-Moulton Integration method and the Newton-Raphson method for correcting the initial estimate of the needed values.

The effects of chemical reactivity, wall temperature as well as the fuel injection rate were investigated with respect to the First Damkohler Number as the independent variable. The results indicate the existence of two types of transition from frozen to equilibrium flow and these are the multi-valued transition and the simple transition. The type of transition depends either on the wall temperature or the injection rate of fuel. The multi-valued transition also yields two critical Damkohler Numbers for the three branches of the solution. If $D_1 >> D_{1,i}$ the system is in equilibrium and if $D_1 << D_{1,e}$ the system is always in the frozen flow region. For D_1 somewhere between $D_{1,i}$ and $D_{1,e}$ the values

of surface heat transfer as well as the fuel concentration at the wall are multi-valued. Depending on the condition at the wall these values can be in the weak burning, middle or strong burning branch.

In the case of multi-valued transition when the system is in the frozen flow region as the First Damkohler Number is increased, by decreasing the free stream velocity of the oxidizing mixture, a value of D_1 will be reached beyond which the reactive process will proceed at a very high rate and the system will reach the equilibrium flow region. The limit of $D_1 = D_{1,i}$ establishes the critical Ignition Damkohler Number. On the other hand when the system is initially in the equilibrium flow region, as D_1 is decreased a limiting value is reached beyond which the system shifts to the frozen flow region. This limit of $D_1 = D_{1,e}$ establishes the critical Extinction Damkohler Number.

In the case of the simple transition, the change from frozen to equilibrium flow and vise versa, occurs through a smooth change in the rate of the reaction process. In this case no distinct limits of ignition and extinction can be established.

The following conclusions have been reached when considering the effects of wall temperature and fuel injection rate:

(a) At low wall temperatures, ignition and extinction occur at high values of D_1. When wall temperature increases

$D_{1,i}$ and $D_{1,e}$ decrease. However, at some values of θ_w the transition from frozen to equilibrium flow becomes simple.

(b) At a fixed wall temperature, low injection rate will lead to a simple transition and high injection rate to a multi-valued transition.

(c) The surface heat transfer and the fuel concentration at the wall are independent of the wall temperature and D_1 for frozen flow, very much dependent on both the wall temperature and D_1 in the transition region, but only dependent on the wall temperature in the equilibrium flow region.

(d) Higher wall temperatures lead to lower values of surface heat transfer at extinction but higher values of $Nu/(Re)^{1/2}$ at ignition.

The location of the reaction zone also depends on D_1 and $\bar{f}_w$. It tends to move towards the wall at low fuel injection rate $\bar{f}_w$, high wall temperatures θ_w and with increasing D_1 values. Study of the effects of injection rate, as discussed before, lead to the prediction that $\bar{f}_w$ must have a value such that the fuel mass fraction in the boundary layer mixture is stoichiometric. The solution, then, will yield a multi-valued transition instead of a simple one.

There remains considerable additional work on this problem which is left from the present work. This work can be (i) an investigation of the effect of oxygen mass fraction

in the free stream, (ii) a study of the effect of temperature in free stream and (iii) an investigation of the effect of activation energy. Finally, any revision of the numerical method might also be of interest.

APPENDIX

In this Appendix eighteen figures have been included to supplement the results presented in the main body of the thesis.

Figures A1 through A4 establish the effects of the fuel injection rate on the surface heat transfer and the fuel mass fraction at the wall at θ_w = 2.5 and 4.5. Figures A5 through A8 compare the effects of wall temperature at the injection rates $\bar{f}_w$ of -0.02 and -0.03. Figures A9 and A10 present temperature profiles for θ_w = 3.0 and 2.5. Figures A11 through A18 present fuel concentration profiles.

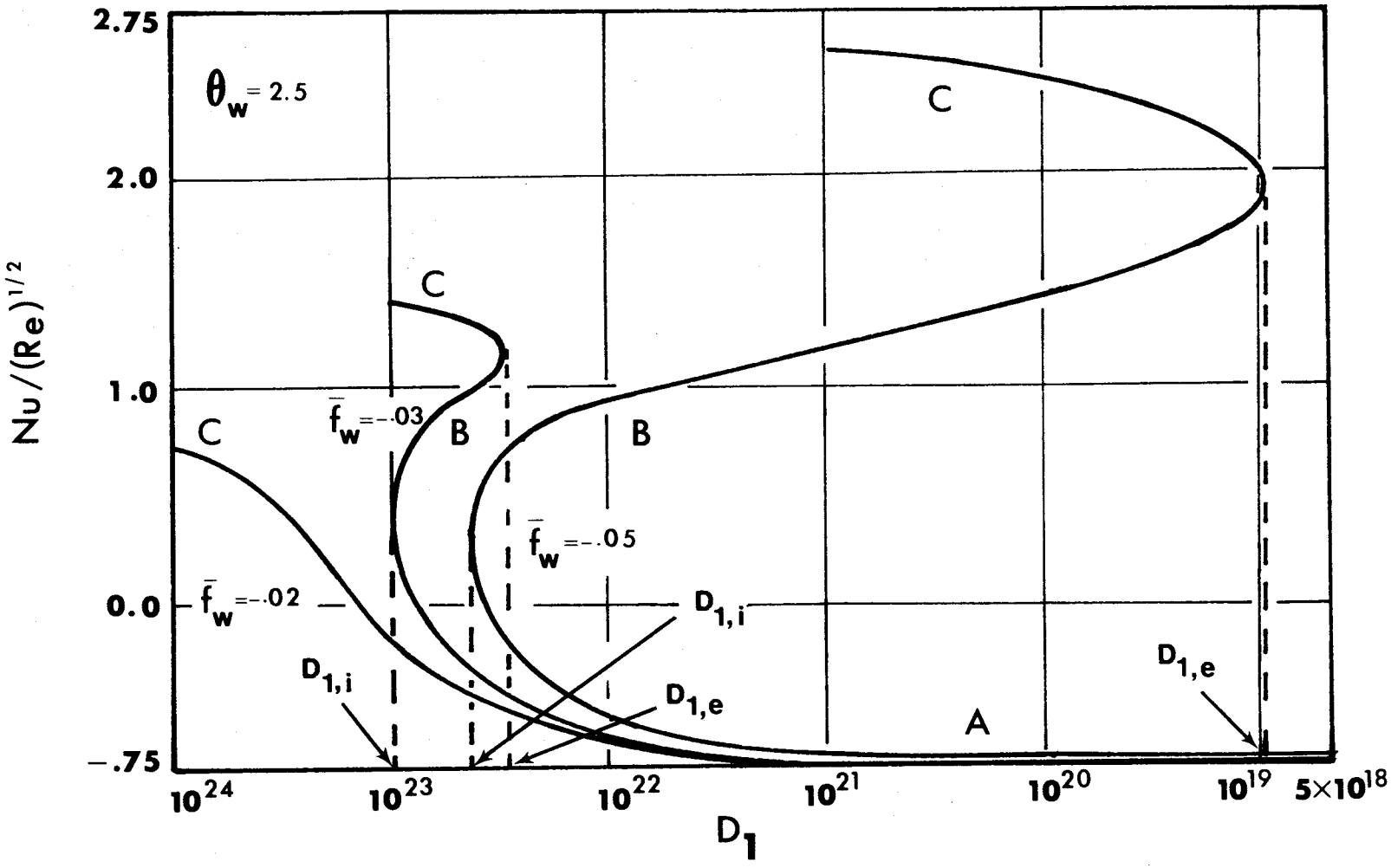

Figure A1. Effect of Injection Rate on Surface Heat Transfer, $\theta_w = 2.5$

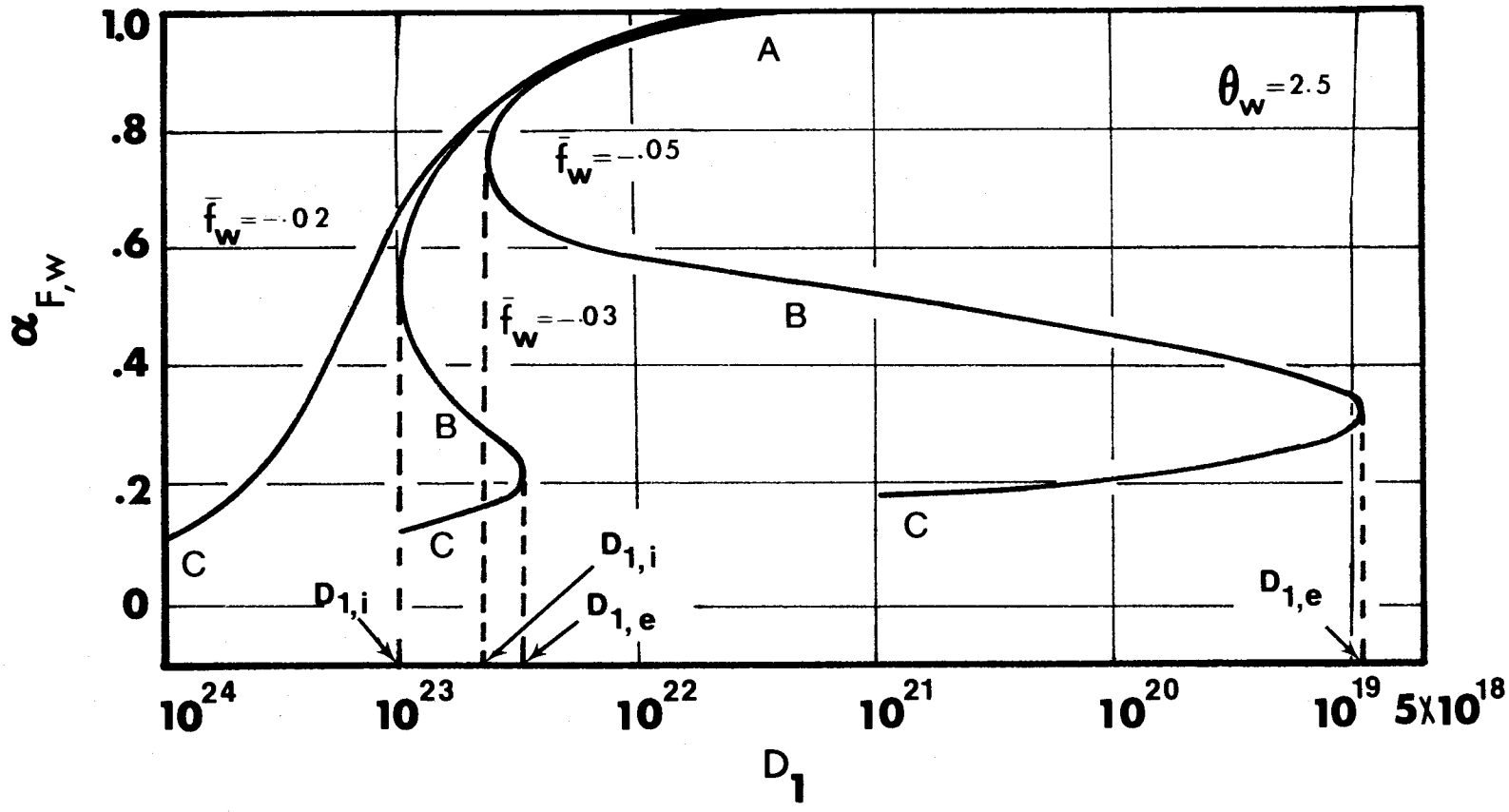

Figure A2. Effect of Injection Rate on Fuel Mass Fraction at the Wall, $\theta_w = 2.5$

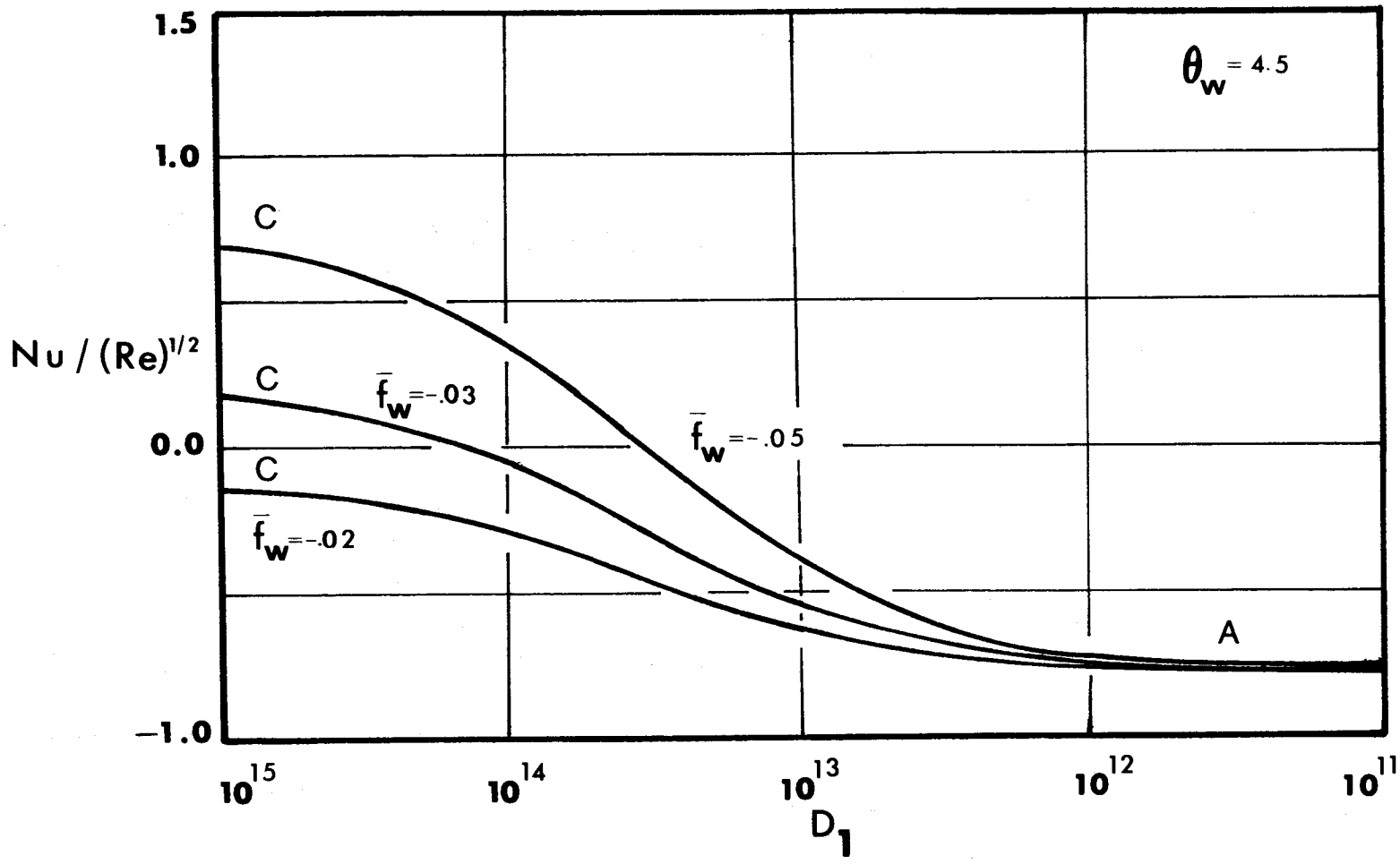

Figure A3. Effect of Injection Rate on Surface Heat Transfer, θ_W = 4.5

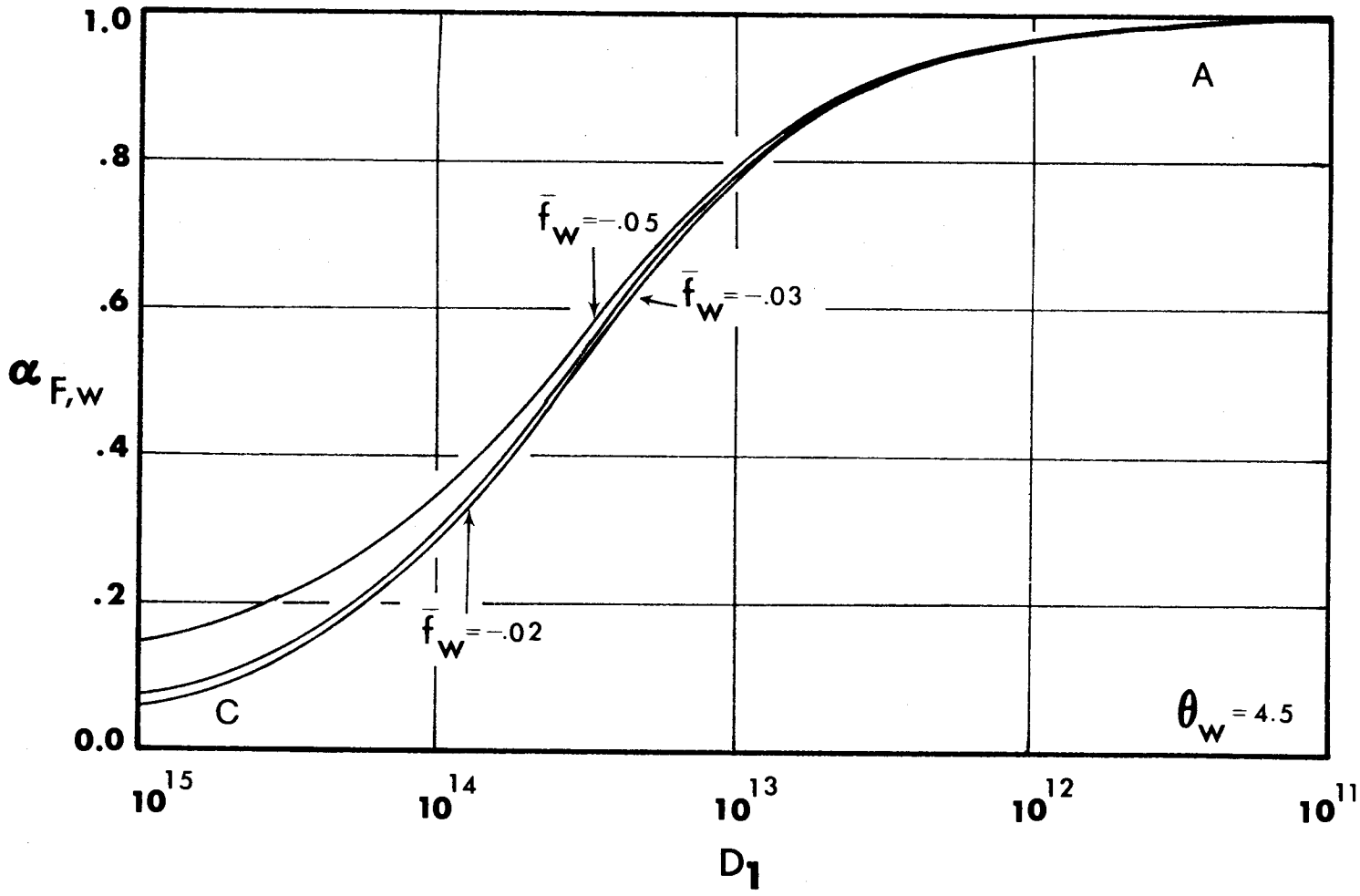

Figure A4. Effect of Injection Rate of Fuel Mass Fraction at the Wall, $\theta_w = 4.5$

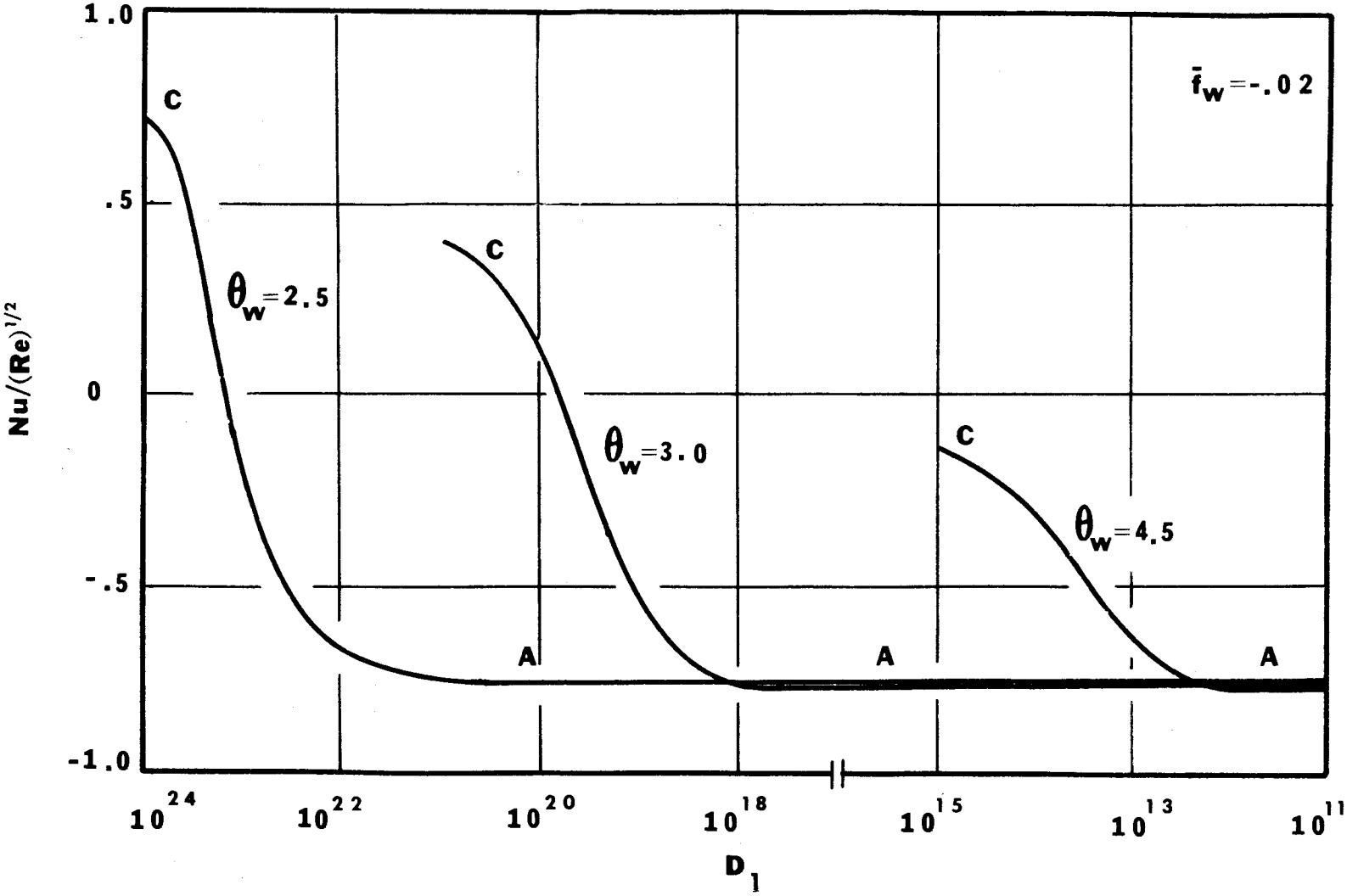

Figure A5. Effect of Wall Temperature on Surface Heat Transfer, $\bar{f}_w$ = -0.02

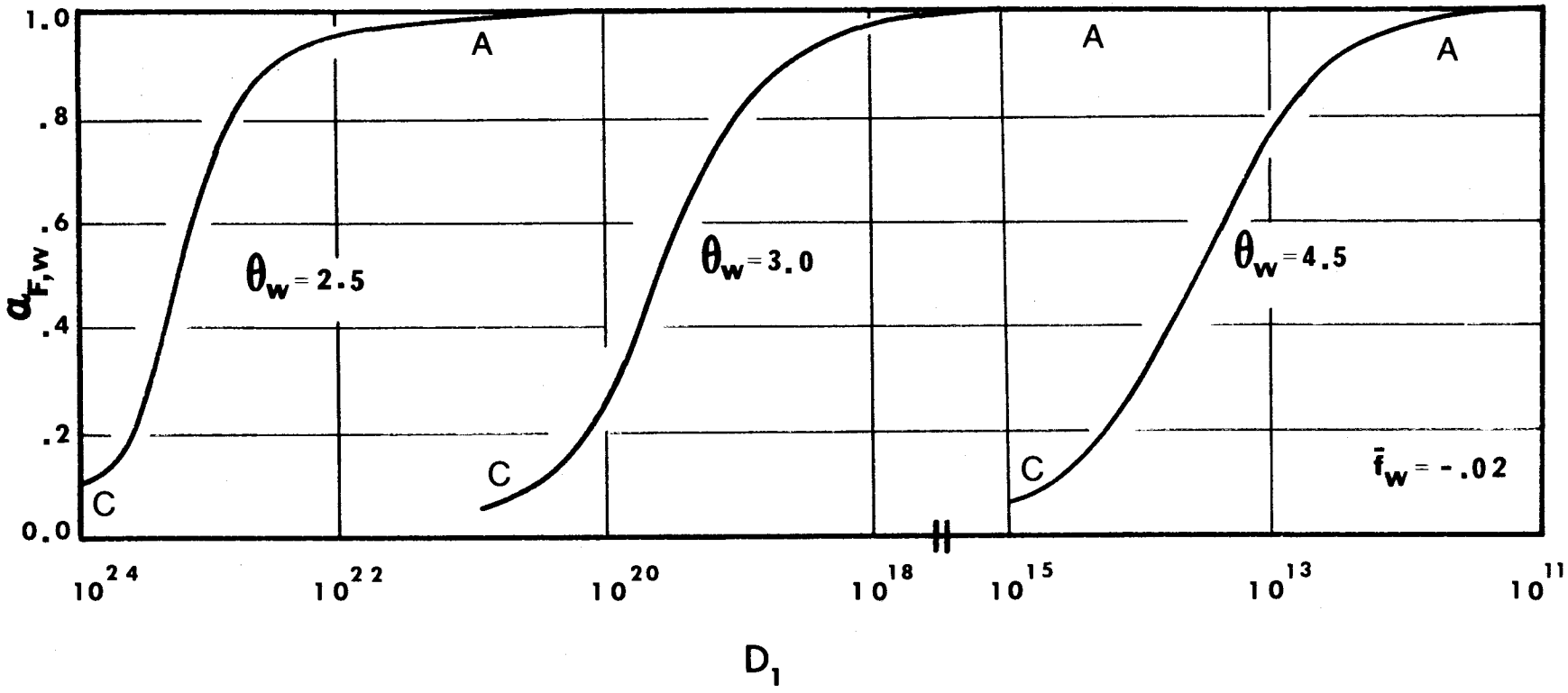

Figure A6. Effect of Wall Temperature on Fuel Mass Fraction at the Wall, $\bar{f}_w = -0.02$

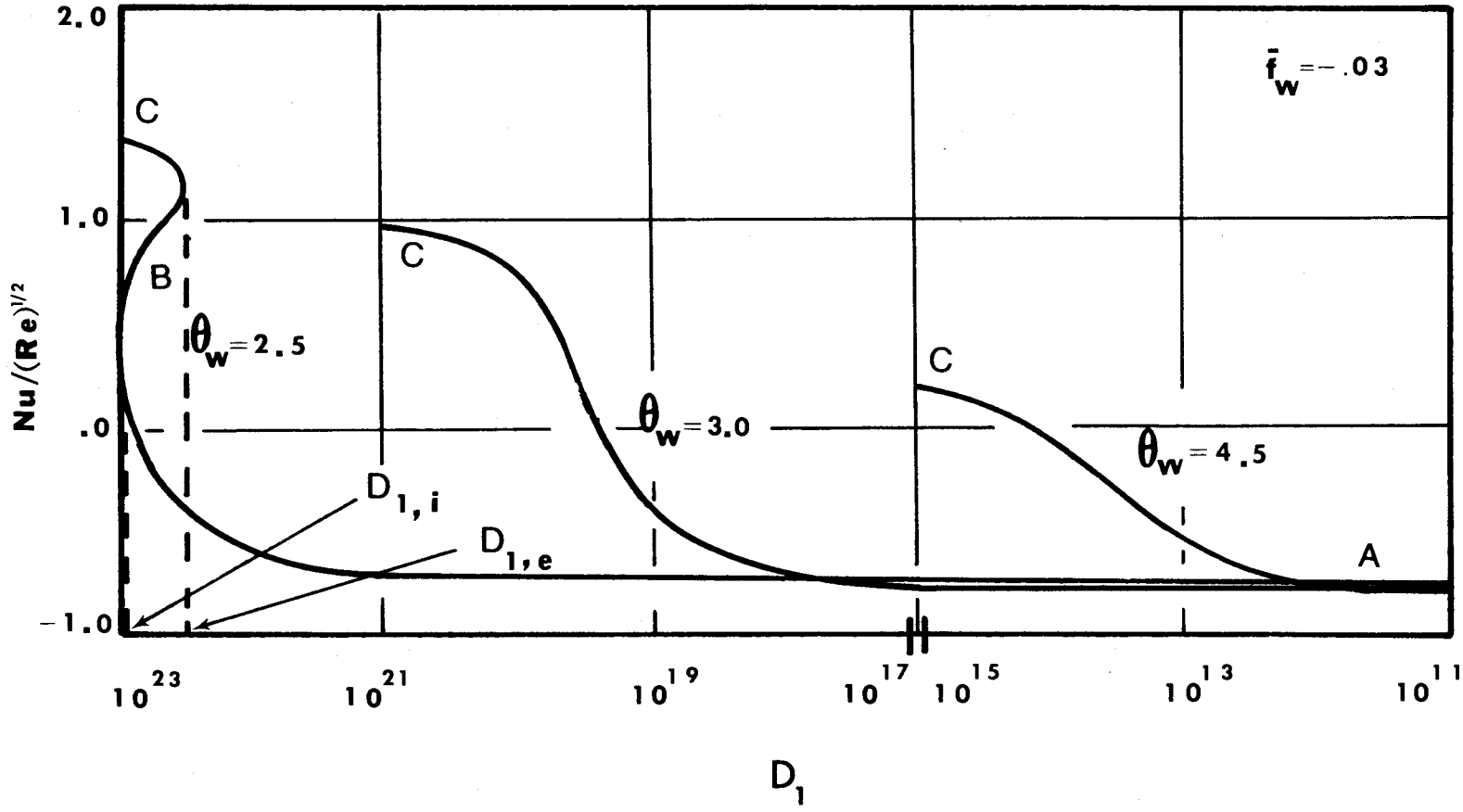

Figure A7. Effect of Wall Temperature on Surface Heat Transfer, $\bar{f}_w$ = -0.03

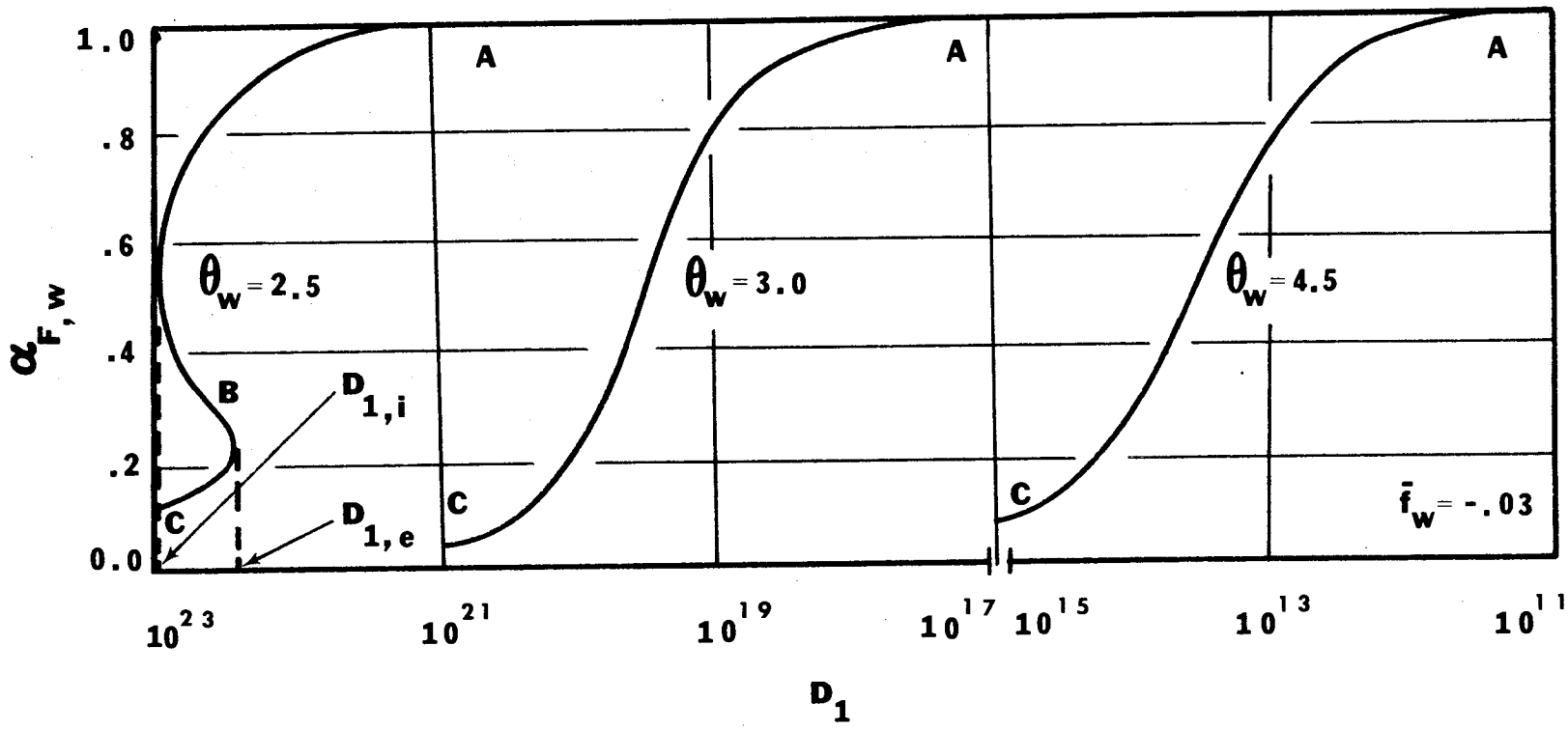

Figure A8. Effect of Wall Temperature on Fuel Mass Fraction at the Wall, $\bar{f}_w = -0.03$

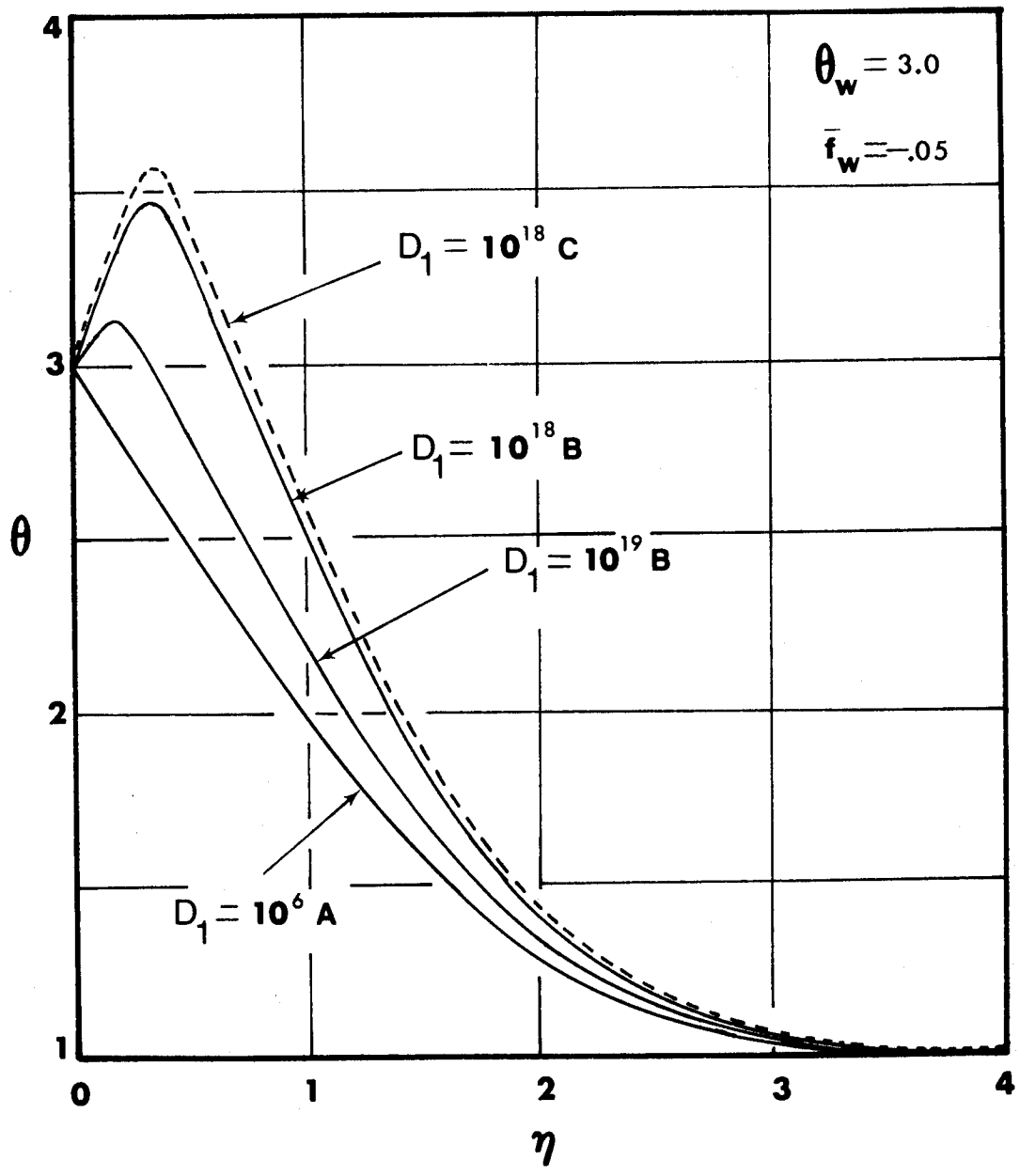

Figure A9. Temperature Profiles at θ_w = 3.0 and $\bar{f}_w$ = -0.05

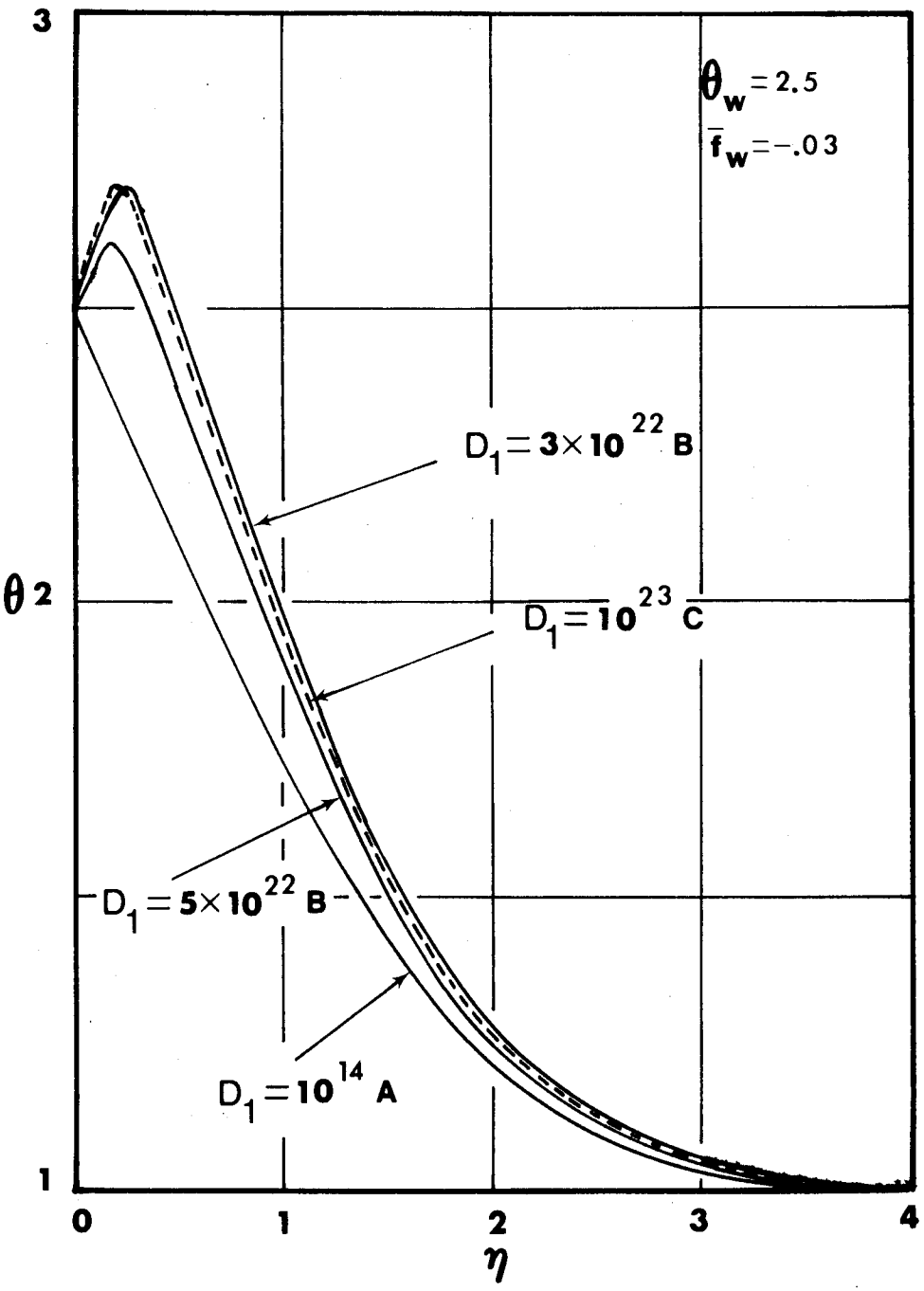

Figure A10. Temperature Profiles at θ_w = 2.5 and $\bar{f}_w$ = -0.03

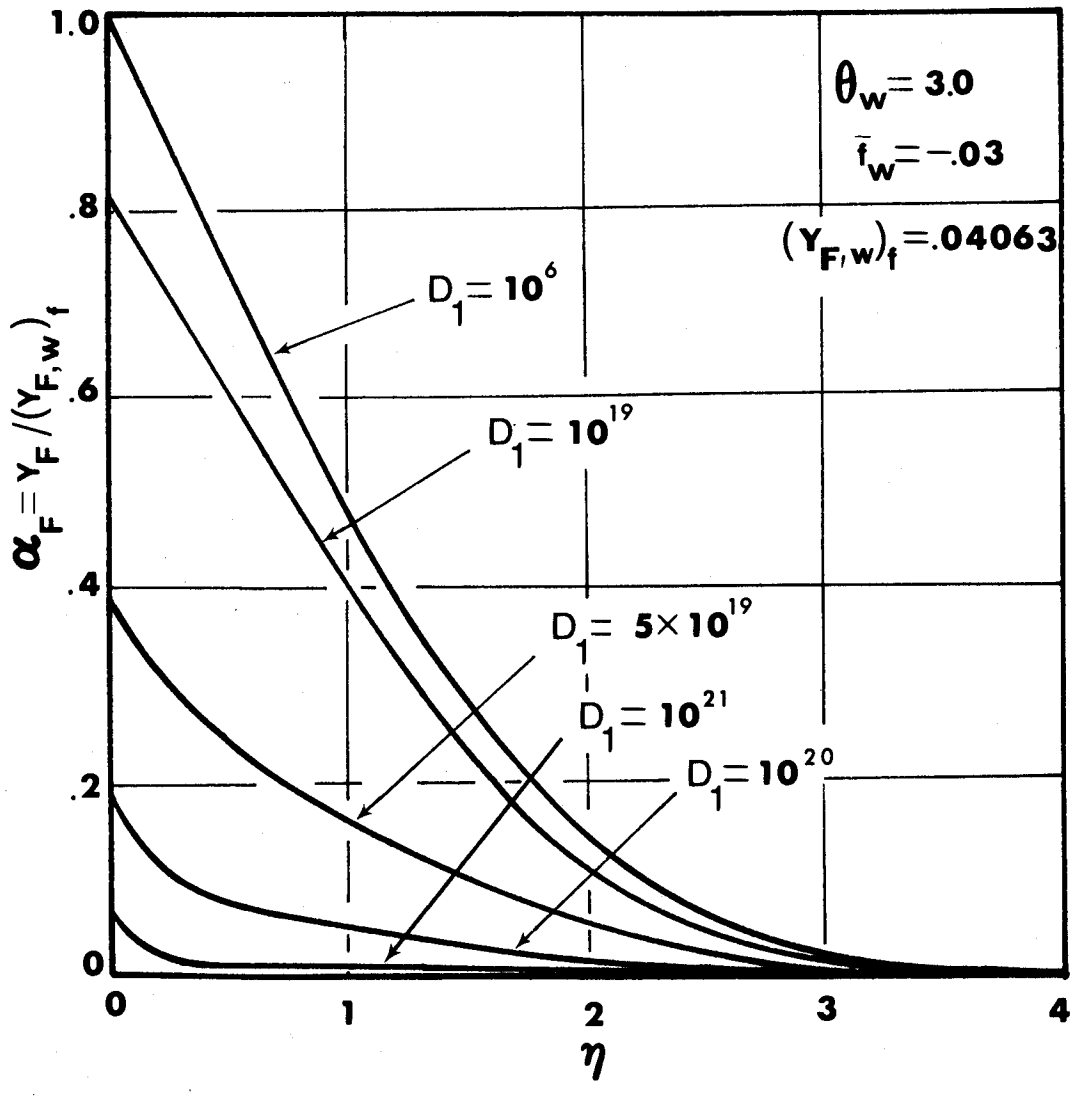

Figure A11. Fuel Mass Fraction Profiles at θ_w = 3.0 and $\bar{f}_w$ = -0.03

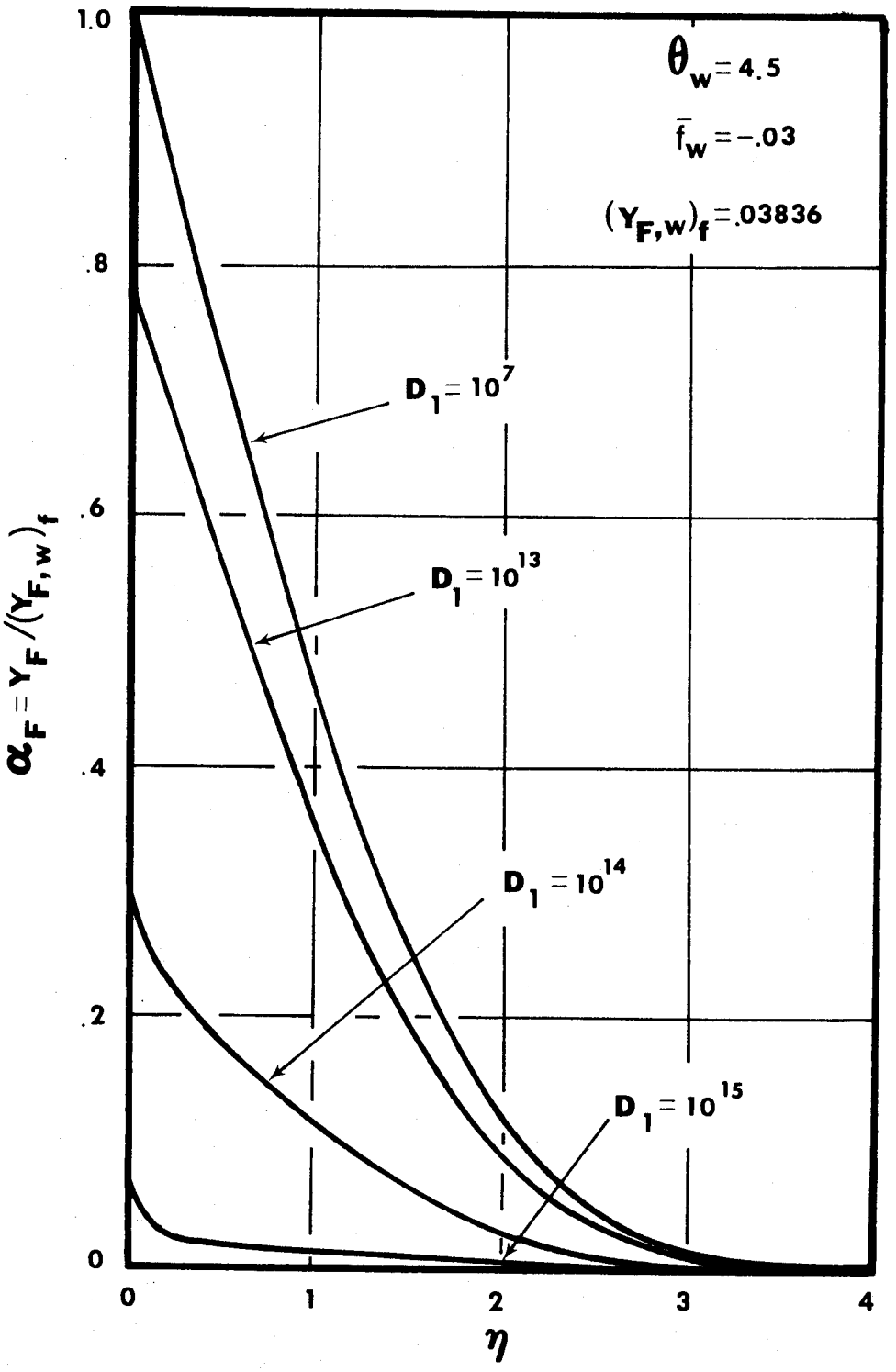

Figure A12. Fuel Mass Fraction Profiles at θ_w = 4.5 and $\bar{f}_w$ = -0.03

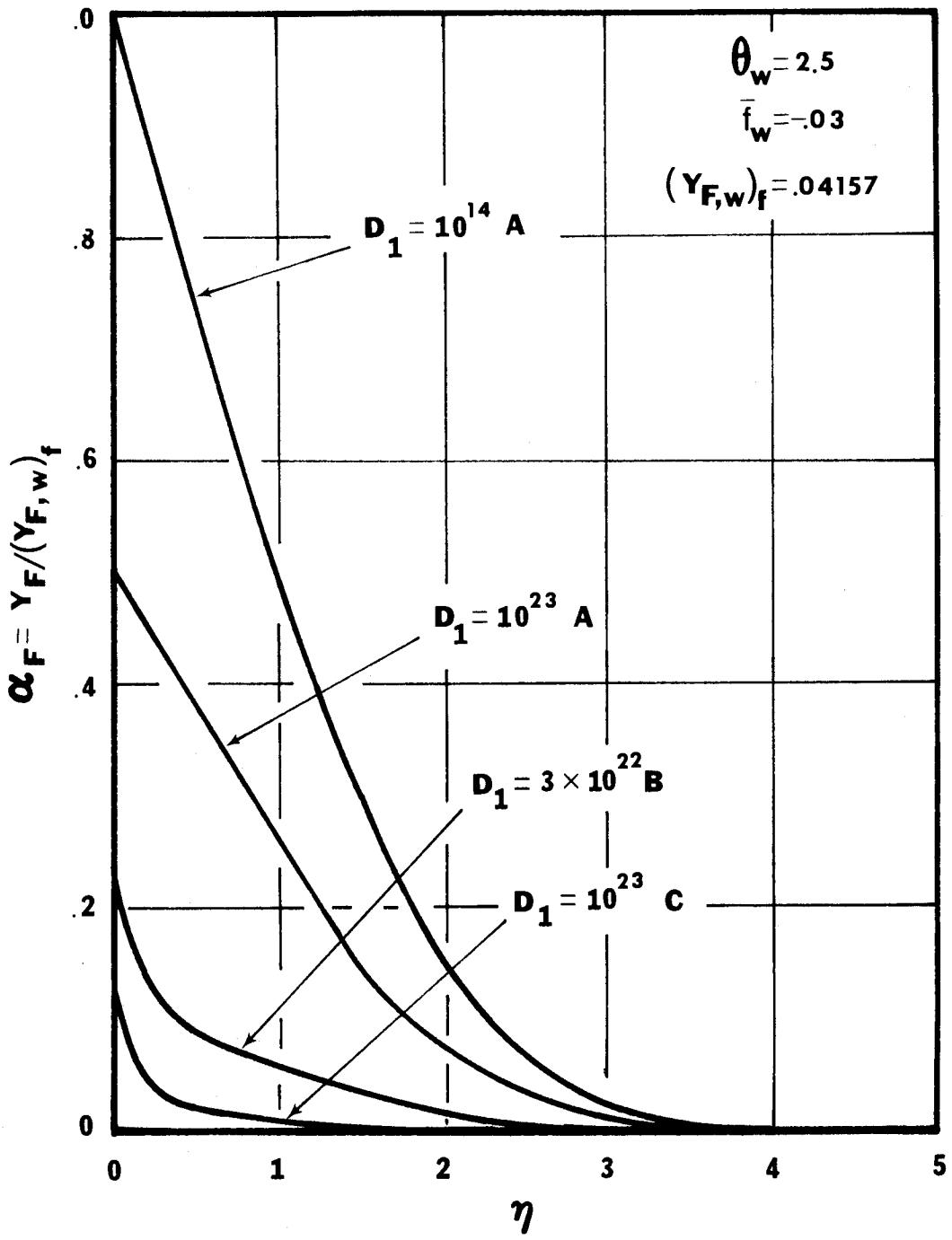

Figure A13. Fuel Mass Fraction Profiles at θ_w = 2.5 and $\bar{f}_w$ = -0.03

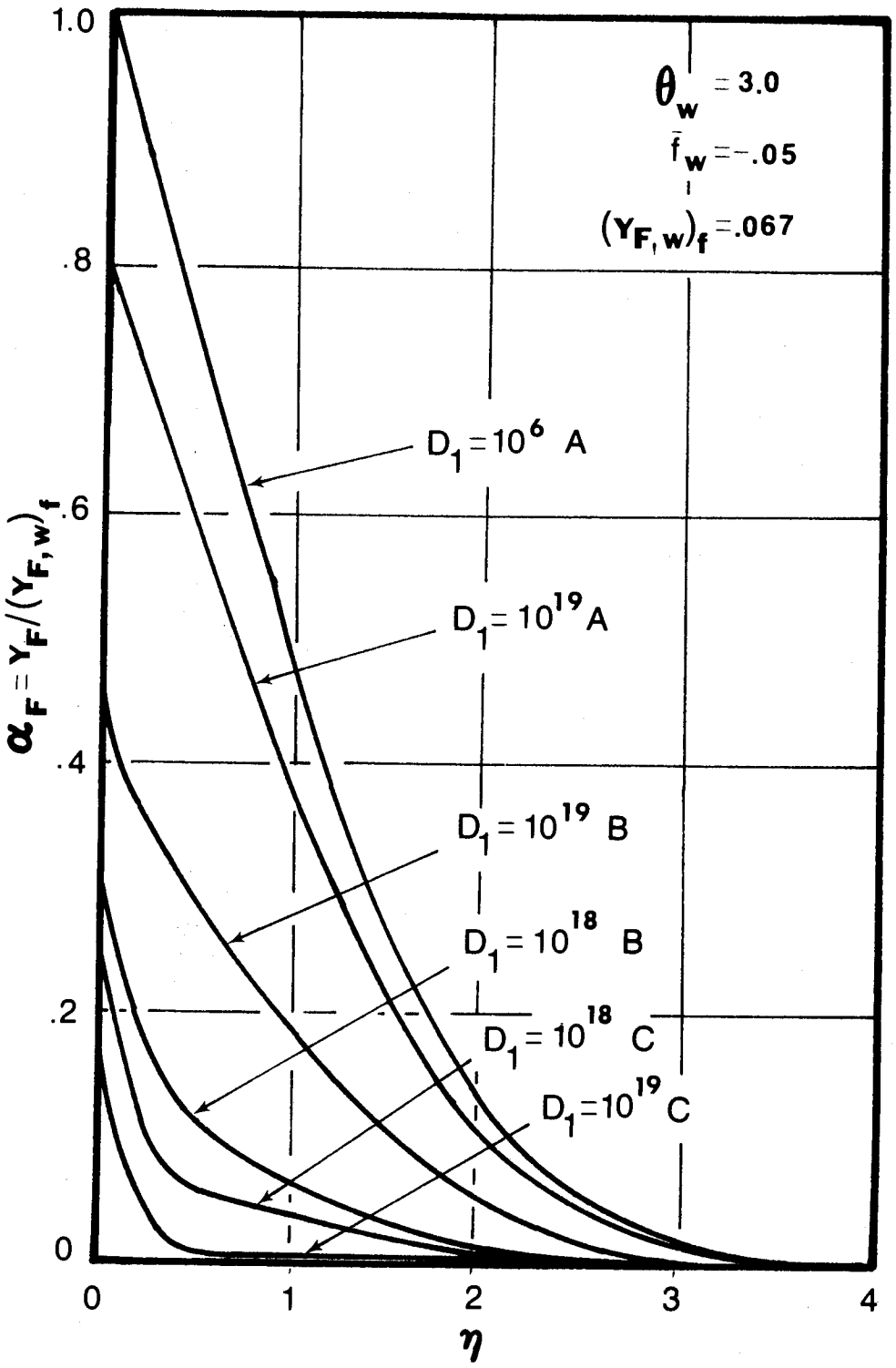

Figure A14. Fuel Mass Fraction Profiles at θ_w = 3.0 and $\bar{f}_w$ = -0.05

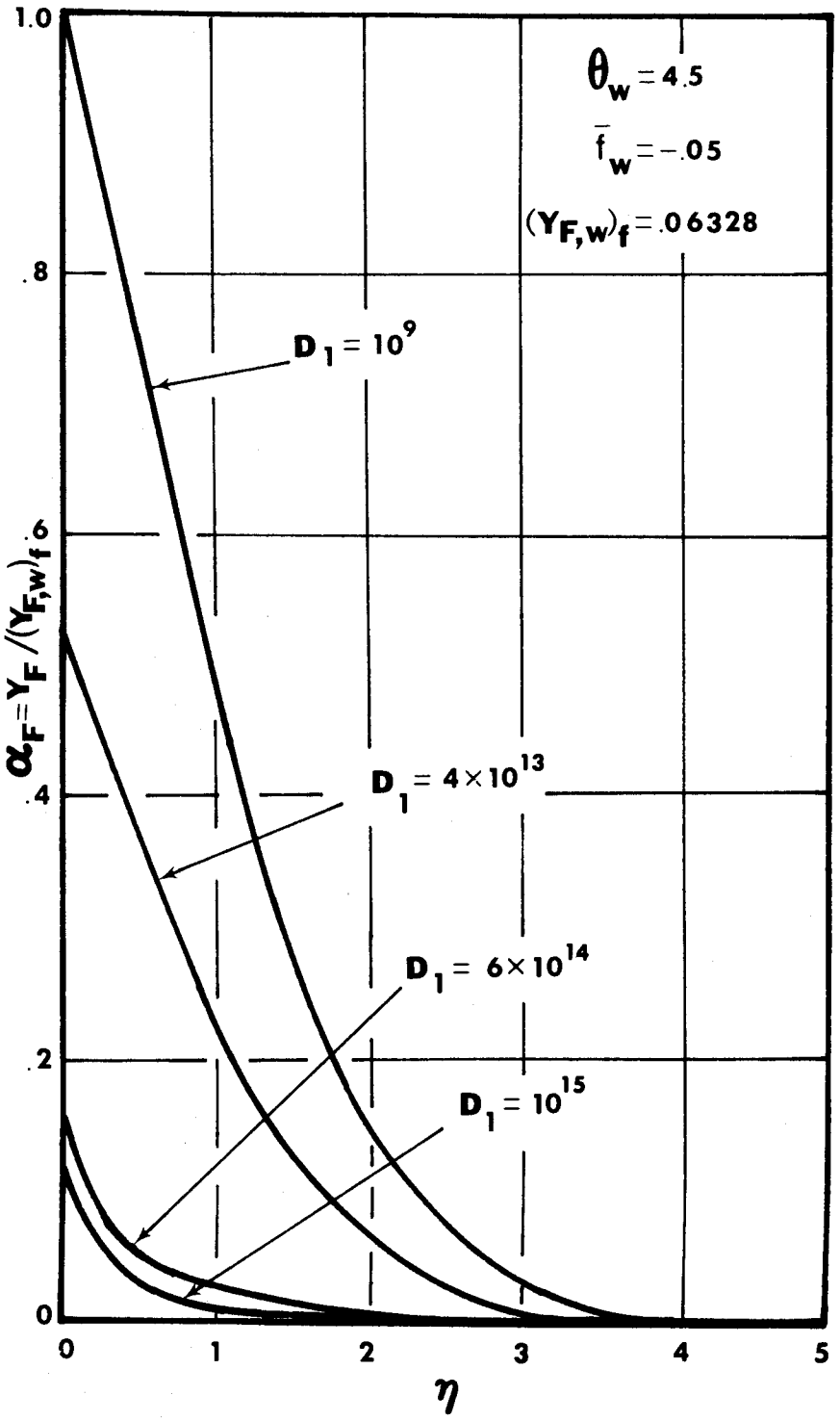

Figure A15. Fuel Mass Fraction Profiles at θ_w = 4.5 and $\bar{f}_w$ = -0.05

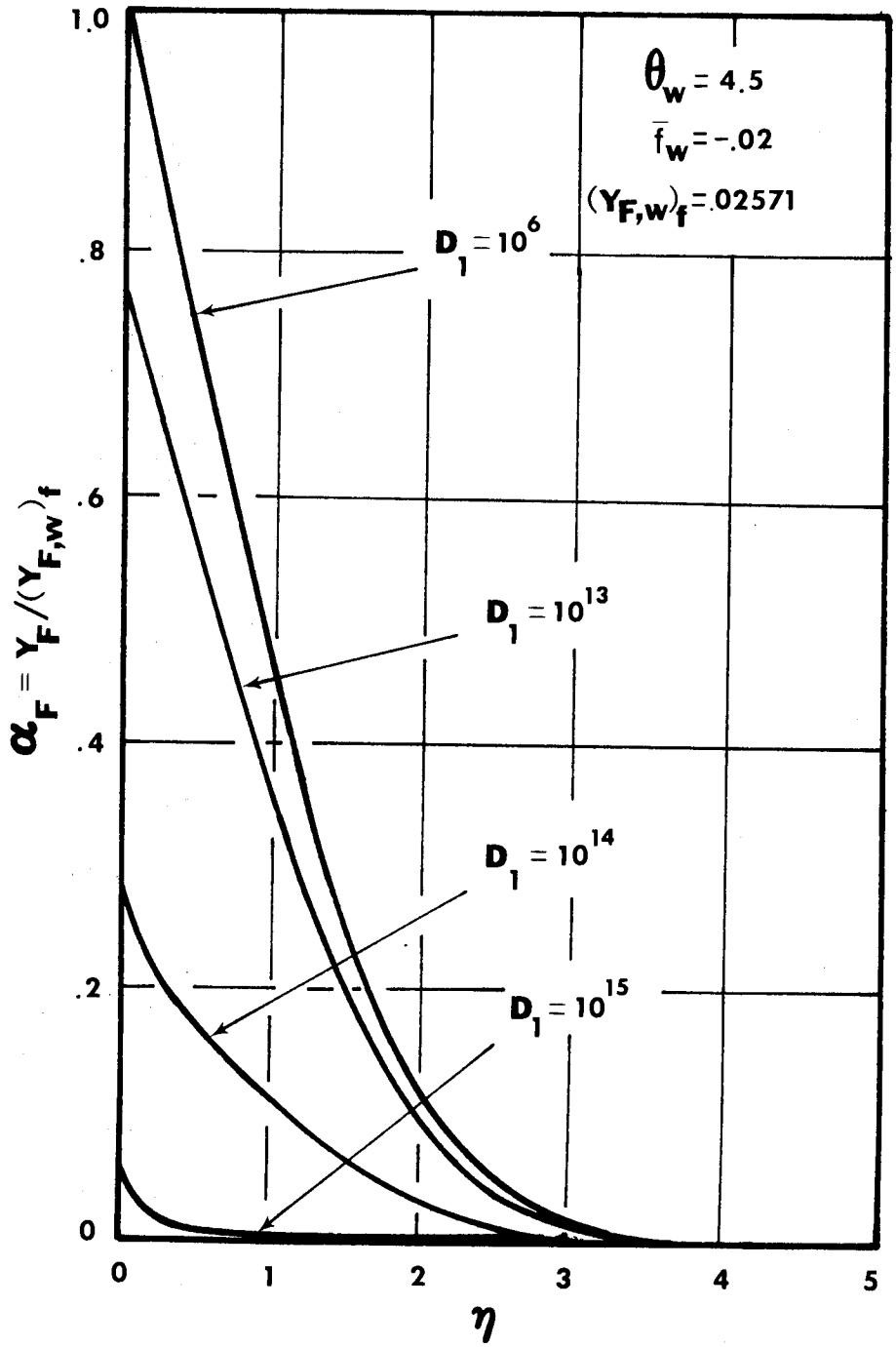

Figure A16. Fuel Mass Fraction Profiles at $\theta_W = 4.5$ and $\bar{f}_W = -0.02$

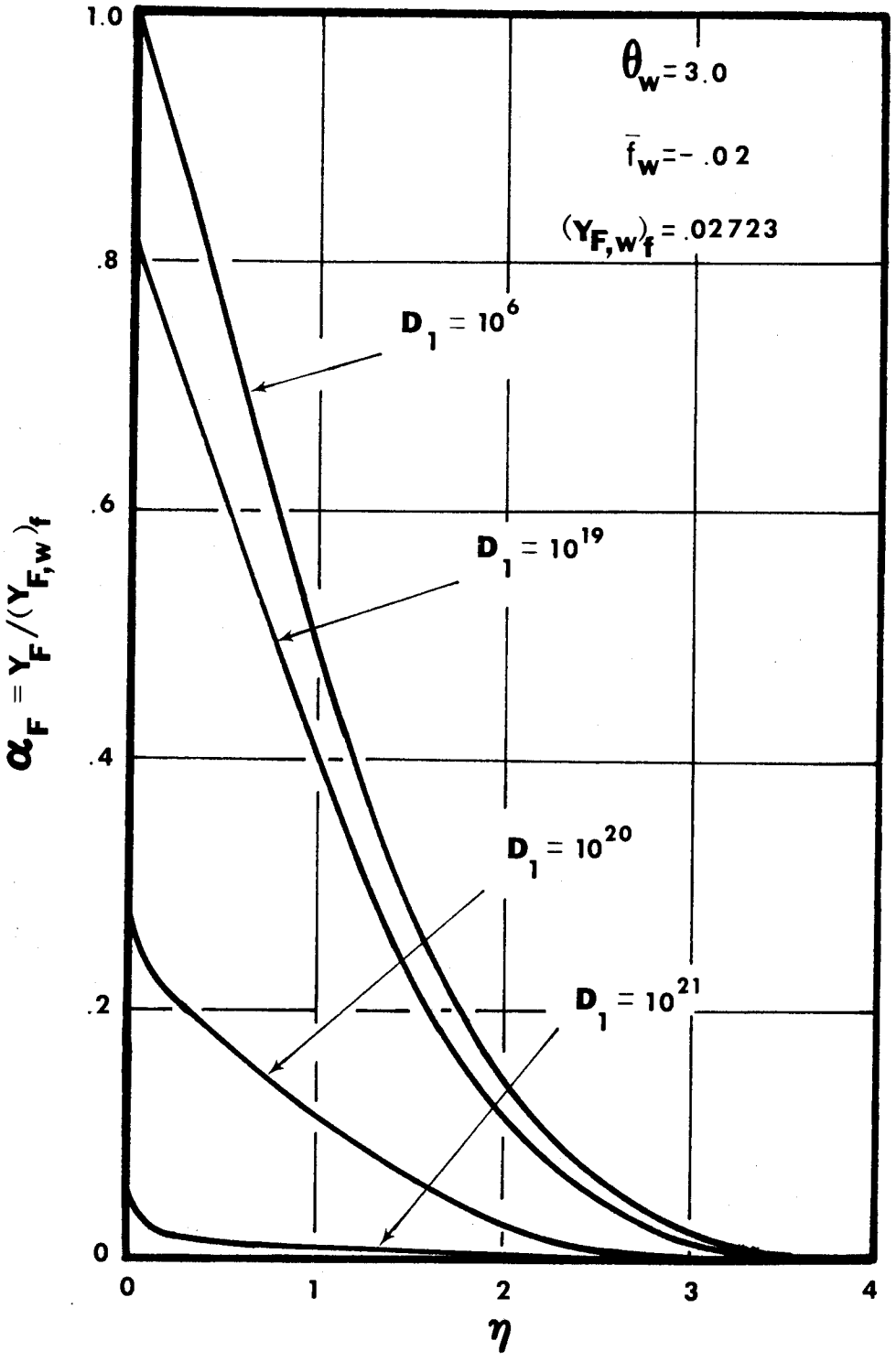

Figure A17. Fuel Mass Fraction Profiles at θ_w = 3.0 and $\bar{f}_w$ = -0.02

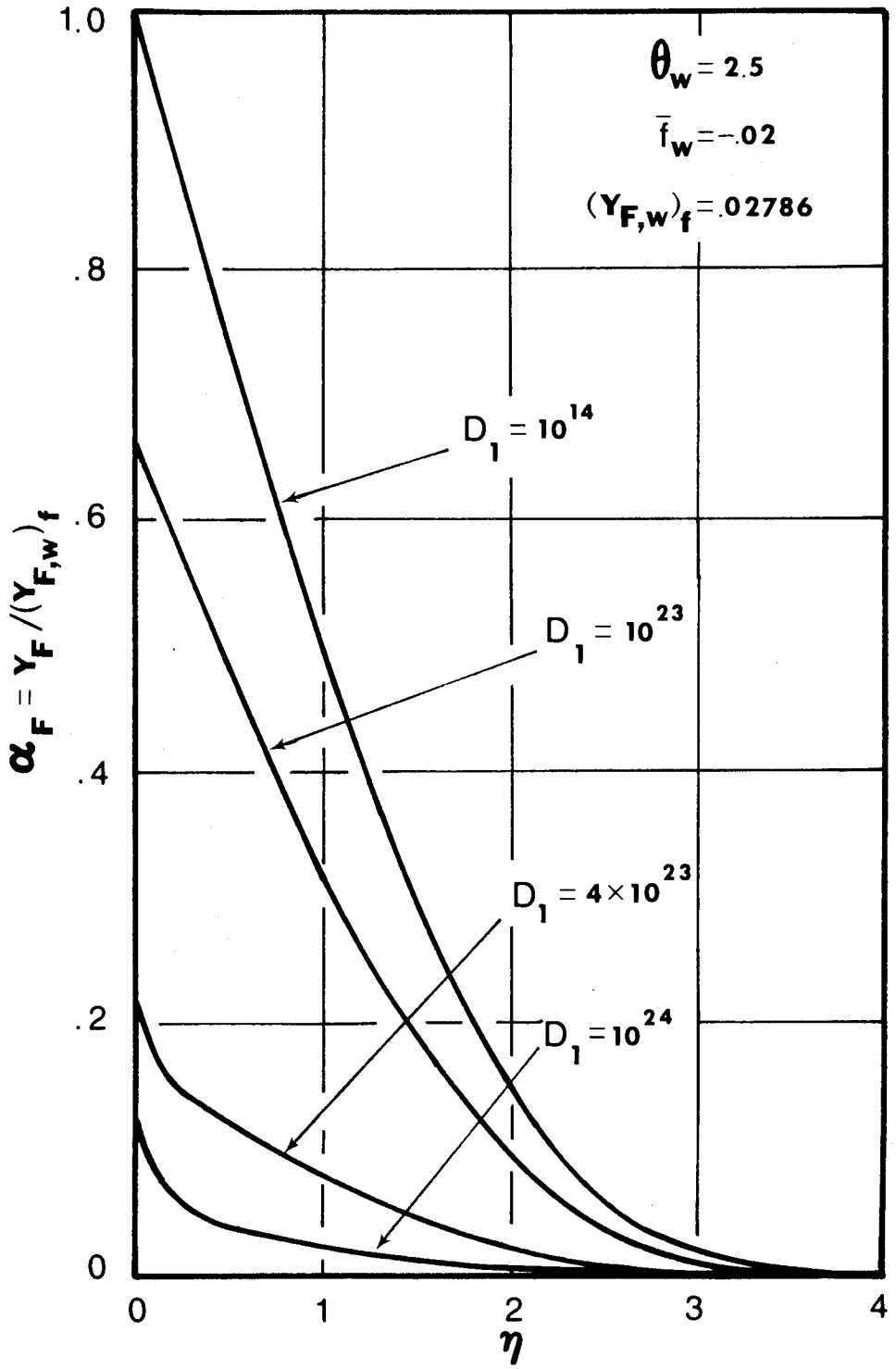

Figure A18. Fuel Mass Fraction Profiles at θ_w = 2.5 and $\bar{f}_w$ = -0.02

REFERENCES

1. Jain, V. K., and Mukunda, H. S., "On the Ignition and Extinction Problem in Forced Convection System," International of Heat and Mass Transfer, Vol. 11, pp. 491-508 (1968).

2. Liu, T. M. and Libby, P. A., "Boundary Layer at a Stagnation Point with Hydrogen Injection," Combustion Science and Technology, Vol. 2, pp. 131-144 (1970).

3. Wu, P. and Libby, P. A., "Further Results on the Stagnation Point Boundary Layer with Hydrogen Injection," Combustion Science and Technology, Vol. 6, pp. 159-168 (1972).

4. Williams, F. A., Combustion Theory, Addison Wesley, Reading (1966).

5. Smith, H. W., Schmitz, R. A., and Ladd, R. D., "Combustion of Premixed System in Stagnation Flow-1 Theoretical," Combustion Science and Technology, Vol. 4, pp. 131-142 (1971).

6. Alkidas, A. and Durbetaki, P., "Ignition of Gaseous Mixture by a Heated Surface," Combustion Science and Technology, Vol. 7, pp. 135-140 (1973).

7. Fendell, F. E., "Ignition and Extinction in Combustion of Initially Unmixed Reactants," Journal of Fluid Mechanics, Vol. 21, pp. 281-303 (1965).

8. Alkidas, A., "The Steady-State Theory of Ignition of Gaseous Mixtures by Hot Surfaces," Ph.D. Thesis, Georgia Institute of Technology (1972).

9. Zeldovich, Y. B., "On the Theory of Combustion of Initially Unmixed Gases," NACA TN 1296 (1951).

10. Marble, F. E. and Adamson, T. C., Jr., "Ignition and Combustion in a Laminar Mixing Zone," Jet Propulsion, Vol. 24, pp. 259-269 (1954).

11. Spalding, D. B., "Theory of Mixing and Chemical Reaction in the Opposed Jet Diffusion Flame," ARS Journal, Vol. 31, pp. 763-771 (1961).

12. Polymeropoulos, C. E. and Peskin, R. L., "Ignition and Extinction of Liquid Fuel Drops-Numerical Computations," Combustion and Flame, Vol. 13, pp. 166-172 (1969).

13. Marathe, A. G. and Jain, V. K., "Some Studies on Opposed Jet Diffusion Flame Considering General Lewis Numbers," Combustion Science and Technology, Vol. 6, pp. 151-157 (1972).

14. Sharma, O. P. and Sirignano, W. A., "Ignition of Stagnation Point Flow by a Hot Body," Combustion Science and Technology, Vol. 1, pp. 95-104 (1969).

15. Alkidas, A. and Durbetaki, P., "Ignition Characteristics of a Stagnation Point Combustible Mixture," Combustion Science and Technology, Vol. 3, pp. 187-194 (1971).

16. Alkidas, A. and Durbetaki, P., "Stagnation Point Heat Transfer: The Effects of the First Damkohler Similarity Parameter," Journal of Heat Transfer, Vol. 94, Series C, pp. 410-414 (1972).

17. Schlichting, H., Boundary Layer Theory, 4th Edition, McGraw-Hill, New York (1960).

18. Eckert, E. R. G. and Drake, R. M., Jr., Analysis of Heat and Mass Transfer, McGraw-Hill, New York (1972).

19. Batchlor, G. K., An Introduction to Fluid Dynamics, Cambridge University Press, New York (1970).

20. Kays, W. M., Convective Heat and Mass Transfer, McGraw-Hill, New York, (1966).

21. Hirschfelder, J. O., Curtiss, C. F., and Bird, R. B., Molecular Theory of Gases and Liquids, John Wiley, New York (1964).

22. Bird, R. B., Stewart, W. E., and Lightfoot, E. N., Transport Phenomena, John Wiley, New York (1960).

23. Laider, K. J., Reaction Kinetics, Vol. 1, Homogeneous Gas Reaction, Pergamon Press, New York (1970).

24. Lees, L., "Laminar Heat Transfer Over Blunt-nosed Bodies at Hypersonic Flight Speed," Jet Propulsion, Vol. 26, pp. 259-269 (1956).

25. Chung, P. M., Fendell, F. E., and Holt, J. F., "Non-equilibrium Anomalies in the Development of Diffusion Flame," AIAA Journal, Vol. 4, pp. 1020-1026 (1966).

26. Nachsteim, D. R. and Paul Swigert, "Satisfaction in Numerical Solution of a System of Non-Linear Equations of Boundary Layer Type," NASA TN D-3004, N 65-35951 (1961).